

THE EFFECT OF SLAG COMPOSITION ON COPPER LOSSES  
TO SILICA-SATURATED IRON SILICATE SLAGS

BARRY JOHN ELLIOT

A Dissertation Submitted to the Faculty of Engineering,  
University of the Witwatersrand, Johannesburg, for the  
Degree of Master of Science in Engineering

Johannesburg 1977

UNDERTAKING

I certify that this is my own work and has not been  
submitted for a Master of Science degree in Engineering at any  
other University

*B. J. Elliot*

B.J. ELLIOT

September 1977

#### ACKNOWLEDGEMENTS

The author thanks the National Institute for Metallurgy for providing the financial assistance which permitted this research to be undertaken as well as the Head of the Department of Metallurgy, Professor R.P. King, for provision of laboratory facilities.

Thanks are extended to Dr. J.B. See for his supervision and encouragement throughout the course of this project as well as to Dr. W.J. Rankin for his general technical assistance and especially his suggestions on the design of the equipment.

Special thanks go to my wife Gabrielle, for preparation of the diagrams and for typing this thesis.

Grateful acknowledgement is made to the Analytical Division of the National Institute for Metallurgy for carrying out the analyses necessary for this investigation.

# ABSTRACT

The effect of fluxing additions of  $\text{MgO}$ ,  $\text{Al}_2\text{O}_3$  and  $\text{CaO}$  on the solubility of copper in silica-saturated iron silicate slag at  $1573^\circ \text{K}$  was studied by contacting copper-gold alloys with the slag in silica crucibles under a partial pressure of oxygen of  $8 \times 10^{-9}$  atm. The oxygen partial pressure was controlled using a  $\text{CO}/\text{CO}_2$  gas mixture.

The results of this investigation confirm that copper is dissolved as  $\text{CuO}_{0.5}$  in silica-saturated fayalite slag. The effect of additions of  $\text{MgO}$ ,  $\text{Al}_2\text{O}_3$  and  $\text{CaO}$  on the solubility of copper in slag was determined by calculating the activity coefficient of  $\text{CuO}_{0.5}$  for each of these flux additions. The activity coefficients of  $\text{CuO}_{0.5}$  in this investigation varied from a minimum of 2.58 for silica-saturated slags without fluxing additions to a maximum of 3.81 for a slag containing 10.5 mass per cent lime. Additions of  $\text{MgO}$  and  $\text{Al}_2\text{O}_3$  slightly increased  $\gamma_{\text{CuO}_{0.5}}$  whilst additions of  $\text{CaO}$  substantially increased  $\gamma_{\text{CuO}_{0.5}}$ . An increase in the activity coefficient at constant activity of copper oxide in the slag results in a decrease in the solubility of copper in the slag.

Equations were also developed to relate the solubility of copper in slag containing either  $\text{MgO}$ ,  $\text{Al}_2\text{O}_3$  or  $\text{CaO}$  to the activity of  $\text{CuO}_{0.5}$  in the slag. The maximum solubility of copper in the slag equilibrated with a Cu-Au alloy ( $a_{\text{Cu}} = 0.80$ ) varied from a maximum of 2.10 mass per cent for slag without fluxing additions to a minimum of 1.40 mass per cent for slag containing 10.5 mass per cent lime.



The variations in the activity coefficients of  $\text{CuO}_{0.5}$  were interpreted using the acid-base theory of slags. This theory confirms that the more basic oxides have a greater effect on the activity coefficient of copper oxide.

The knowledge obtained in this investigation of the effects of fluxing additions on the solubility of copper in the slag will be helpful in choosing optimum compositions for copper smelting slags to reduce chemical copper losses to these slags.

## TABLE OF CONTENTS

	PAGE
1. INTRODUCTION	1
2. PREVIOUS WORK	2
2.1 Forms of copper losses to slag	2
2.2 Factors affecting copper losses to slag	3
2.3 Parameters affecting copper solubility in slag	4
2.3.1 Oxygen partial pressure	4
2.3.2 Temperature	12
2.3.3 Slag composition	12
2.3.3.1 Iron	14
2.3.3.2 Alumina	17
2.3.3.3 Magnesia	19
2.3.3.4 Lime	19
2.3.4 Summary and comparison of different investigations	21
3. EXPERIMENTAL	25
3.1 Experimental design	25
3.2 Basic experimental procedure	28
3.3 Materials	29
3.3.1 Slag	30
3.3.2 Alloy	32
3.3.3 Crucible material	37
3.4 Apparatus	38
3.4.1 Gas train	38
3.4.2 Furnace assembly	44
3.5 Procedure	49
3.6 Analytical techniques	51
3.6.1 Preparation of samples for analysis	51
3.6.2 Analysis of alloy	52
3.6.3 Analysis of slag	53

<u>TABLE OF CONTENTS</u> (cont.)	PAGE
4. RESULTS	55
4.1 Equilibration time	55
4.2 Copper solubility in iron silicate slag	57
4.3 Copper solubility in iron silicate slag with fluxing additions	59
5. SOLUBILITY OF COPPER IN SILICA-SATURATED IRON SILICATE SLAGS	64
5.1 No fluxing additions	64
5.1.1 Solubility of copper as $\text{CuO}_{0.5}$	66
5.1.2 Activity of $\text{CuO}_{0.5}$	69
5.1.3 Prediction of solubility of copper	75
5.2 Effect of fluxing additions	77
5.2.1 Magnesia	77
5.2.2 Alumina	86
5.2.3 Lime	92
5.3 Practical implications of results	97
6. FUTURE WORK	99
7. CONCLUSIONS	101
8. REFERENCES	103
9. APPENDIX	110

<u>LIST OF FIGURES</u>	PAGE
1. Copper Oxide in Slag Versus Oxygen Partial Pressure for Silica-Saturated Iron Silicate Slags	6
2. Relation Between Copper in Slag and Activity of Copper in the Alloy	9
3. Copper Solubility in Slag as a Function of Copper Oxide Activity from Taylor and Jeffes (22)	11
4. Effect of Temperature on the Solubility of Copper in Slag at $p_{O_2} = 10^{-8}$ atm from Toguri and Santander (20)	13
5. Ratio of Copper to Iron in Slag Versus Partial Pressure of Oxygen at $1573^{\circ}$ K (16)	15
6. Copper in the Slag Versus Oxygen Partial Pressure for Higher Iron Slags from Bailey (16)	16
7. Copper in the Slag Versus Oxygen Partial Pressure for Silica-Saturated Slags from Bailey (16)	20
8. Partial Liquidus Diagram for the System $FeO-Fe_2O_3-SiO_2$ (14)	31
9. Liquidus Diagram for the System $MgO - "FeO" - SiO_2$ (31)	33
10. Liquidus Diagram for the System $"FeO" - Al_2O_3 - SiO_2$ (31)	34
11. Liquidus Diagram for the System $CaO - "FeO" - SiO_2$ (31)	35
12. Activities in Cu-Au Liquid Solutions at $1550^{\circ}$ K (35)	36
13. Schematic flowsheet for Alloy-Slag Equilibration System	39

LIST OF FIGURES cont.

PAGE

14. Furnace Assembly	45
15. Reaction Tube Arrangement	47
16. Crucible Arrangement	48
17. Schematic Diagram of Electrical Circuit Used for Alloy-Slag Equilibrations	50
18. Copper Dissolved in Silica-Saturated Slag as a Function of Contacting Time	56
19. Gold Content of Slag for Different Runs	58
20. Solubility of Copper in Silica-Saturated Slag	65
21. Activity Coefficients of $\text{Cu}_2\text{O}$ and $\text{CuO}_{0,5}$ Versus Mole Fractions of $\text{Cu}_2\text{O}$ and $\text{CuO}_{0,5}$	68
22. Activity Coefficient of Copper Oxide as a Function of Mole Fraction of Copper Oxide in Silica-Saturated Slag Without Fluxing Additions	74
23. Relationship Between Mass Per Cent Copper Oxide in Slag and $a_{\text{CuO}_{0,5}}$ at $1573^\circ \text{K}$ for Silica-Saturated Slag Without Fluxing Additions	76
24. Solubility of Copper in Silica-Saturated Slag Containing $\text{MgO}$	78
25. Activity Coefficient of Copper Oxide as a Function of Mole Fraction of Copper Oxide in Silica-Saturated Slag Containing 4 Mass Per Cent Magnesia	80

LIST OF FIGURES cont.

PAGE

- |     |   |     |
|-----|---|-----|
| 26. | Relationship Between Mass Per Cent Copper and $a_{\text{CuO}_{0.5}}$<br>in Silica-Saturated Slag Containing<br>4 Mass Per Cent MgO at 1573° K                     | 81  |
| 27. | Solubility of Copper in Silica-Saturated Slag<br>Containing $\text{Al}_2\text{O}_3$   | 87  |
| 28. | Activity Coefficient of Copper Oxide as a Function of<br>Mole Fraction of Copper Oxide in Silica-Saturated Slag<br>Containing Alumina                             | 89  |
| 29. | Relationship Between Mass Per Cent Copper and $a_{\text{CuO}_{0.5}}$<br>in Silica-Saturated Slag Containing<br>8 Mass Per Cent $\text{Al}_2\text{O}_3$ at 1573° K | 90  |
| 30. | Solubility of Copper in Silica-Saturated Slag<br>Containing CaO   | 93  |
| 31. | Activity Coefficient of Copper Oxide as a Function of<br>Mole Fraction of Copper Oxide in Silica-Saturated Slag<br>Containing Lime                                | 95  |
| 32. | Relationship Between Mass Per Cent Copper and $a_{\text{CuO}_{0.5}}$<br>in Silica-Saturated Slag Containing<br>4,5 , 7,5 and 10,5 Mass Per Cent Lime at 1573° K   | 96  |
| 33. | Calibration Curve for Estimation of Oxygen Partial<br>Pressure  | 112 |

### LIST OF PLATES

### PAGE

1.	Experimental System - Front View	40
2.	Experimental System - Side View	41
3.	Crucible Assembly	48

### LIST OF TABLES

2.1	Summary of Investigations on Copper Solubility in Slag	22-23
3.1	Variation of Silica and $\text{Fe}^{3+}$ Contents and $\text{Fe}^{3+}/\text{Fe}^{2+}$ Ratio with Partial Pressure of Oxygen	43
4.1	Copper Content of Slag for Different Contacting Times	55
4.2	Presentation of Raw Data for Alloy and Slag Composition	61-63
5.1	Activities and Activity Coefficients of $\text{CuO}_{0.5}$ for Alloy and Slag	71-73
5.2	Acid-Base Classification of Oxides	83
A.1	Calibration Table for $\text{CO}_2/\text{CO}$ Flowrates	111

## 1. INTRODUCTION

Smelting of sulphides is the most widely used process for the production of copper and as much as 15% of the metal in the original ore is lost in the overall extraction process. The loss of copper during smelting is about 3% of the copper in the original ore and most of this smelting loss is to the slag.

Copper losses to the slag occur by chemical solution of the metal as the oxide or sulphide or from mechanical entrapment of alloy or matte particles. The most important factors contributing to the chemical losses are the oxygen potential of the slag, temperature, and the slag composition. The effect of oxygen potential and temperature on copper losses has been fairly thoroughly investigated. Little information is available on the effect of slag composition on copper losses to slag. Hence the object of this study was to examine the effect of additions of magnesia, alumina and lime on the solubility of metallic copper in a silica-saturated iron silicate slag. A knowledge of the variations in copper solubility for additions of slag constituents will help in the optimization of flux additions to minimise copper losses to the slag.

In a sulphur-free system, silica-saturated iron silicate slags were equilibrated with copper-gold alloys under a fixed oxygen partial pressure of  $8 \times 10^{-9}$  atm at 1573° K. The copper solubilities in the slags were determined. The results have been interpreted in terms of the theory of the structure of slags.



## 2. PREVIOUS WORK

### 2.1 Forms of Copper Losses to Slag

There is still strong disagreement about the relative proportions of dissolved and entrained copper losses to slags in copper smelting (1, 2, 3, 4, 5). Techniques used to establish the amounts of entrained losses include centrifuging (6,7) and settling (8). Losses by entrapment have been shown to vary from as much as 80 per cent (9, 10) to as little as 25 per cent (7) of the copper losses to the slag. Yazawa and Kamada (11) studied the Cu-Fe-S-SiO<sub>2</sub>-CaO system and found that copper in solution represented about half the loss of copper to the slag.

In 1968 Young (12) attempted to clarify the mechanisms and nature of copper losses to slags by a reassessment of earlier work using more recent information. It was concluded that the evidence for exsolution (formation of copper globules in the slag by dissolution of the immediate area of copper) from the melt was still indirect and further work was required. From a mineralogical investigation Young (12) concluded that the major proportion of the copper in reverberatory slag is present as a submicron dispersion of sulphides which was not positively identified. However, readily identifiable larger globules seemed to have been formed by an exsolution and agglomeration process. Recent investigations support the view that a major portion of the unrecovered copper is in true solution in the slag. The two most important developments have been the determination of the extent of oxidic and sulphidic (13) dissolution of copper.

## 2.2 Factors Affecting Copper Losses to Slag

A number of factors influence the losses of copper in smelting slags (1, 2, 3) Thermodynamic factors have an important influence on copper losses to slag and these factors include:

1. Matte grade
2. Magnetite content of slag
3. Oxygen potential of the slag - measured by the  $\text{Fe}^{3+}/\text{Fe}^{2+}$  ratio of the slag
4. Oxygen content of the matte
5. Slag composition -  $\text{SiO}_2$ , total iron,  $\text{CaO}$ ,  $\text{Al}_2\text{O}_3$ ,  $\text{MgO}$
6. Temperature

Physical properties that influence losses of copper to slag include melting point, viscosity, density and surface tension of the slag. The other important factors are associated with operating practice - slag-to-blister ratio, converter slag recycling and the flow characteristics of the furnace.

Toguri, Themelis and Jennings (14) emphasized that to clarify the relative magnitudes of copper losses by entrainment and solution, further research was needed into the effect of oxygen pressure and minor slag components on copper solubility in iron silicate slags. Subsequently a number of fundamental studies have been reported on the effect of atmosphere and slag composition on copper solubility in synthetic slags. These reports are reviewed in the next section.

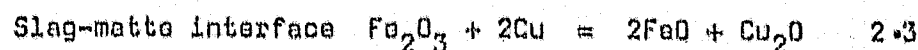
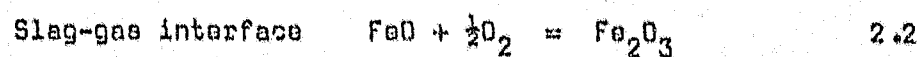
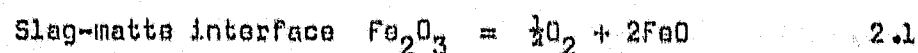
### 2.3 Thermodynamic Factors Affecting Copper Solubility in Slags

#### 2.3.1 Oxygen Partial Pressure

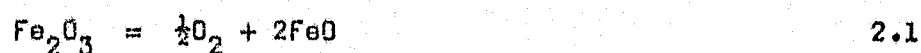
The effect of oxygen partial pressure on copper solubility has been appreciated since the early sixties. Ruddle, Taylor and Bates (8) first demonstrated the variation of the solubility of copper in a silica-saturated iron silicate slag in equilibrium with pure copper under a CO/CO<sub>2</sub> atmosphere. Similar systems were used by Mihalop (15), Bailey (16) and Toguri and Santander (17) to firmly establish this relationship. The results of these earlier investigators were confirmed by Altman and Kellogg (18) who used a technique in which the gas phase was allowed to come to equilibrium with the melt rather than vice versa as per the earlier studies, and Taylor and Jeffes who used the levitation technique to avoid slag contamination by the crucible.

Ruddle et al (8) showed that there was a strong correlation between the Cu<sub>2</sub>O content in the slag and the oxygen partial pressure. This relationship was very similar to that between the ferric oxide content of the slag and the oxygen partial pressure. Therefore, for cases in which equilibrium is not attained between the gas and the liquid phases, as in general smelting practice, the ferric oxide content can be used to indicate the state of oxidation in the slag (19).

Ruddle et al proposed a tentative reaction mechanism for the dissolution of copper in slag by the sequence of reactions:



Reaction 2.3 can be regarded as being the sum of the two reactions



where

$$K_3 = \frac{a_{\text{FeO}}^2 a_{\text{Cu}_2\text{O}}}{a_{\text{Cu}}^2 a_{\text{Fe}_2\text{O}_3}} \quad 2.5$$

Mihalop and Schuhmann (19) argued that for silica-saturated slags  $a_{\text{FeO}}$  is nearly independent of oxygen partial pressure and as the activity of copper in pure metal is unity

$$\frac{a_{\text{Cu}_2\text{O}}}{a_{\text{Fe}_2\text{O}_3}} \approx \text{constant}$$

This illustrates the relationship between copper content of slag and  $\text{Fe}_2\text{O}_3$  content.

Mihalop (15) repeated the work of Ruddle et al (8) and adopted the same reaction mechanism for copper dissolution. Mihalop's results for the solubility of copper in silica-saturated iron silicate slags agree closely with those of Ruddle et al except at higher oxygen partial pressures near  $10^{-6}$  atm (16) (not shown on Figure 1.) where the values are somewhat higher. Mihalop derived the empirical relationship

$$\% \text{Cu}_2\text{O} = 159.6 p_{\text{O}_2}^{0.21} \quad 2.6$$

which compares with the relationship of Ruddle et al

$$\% \text{Cu}_2\text{O} = 125.6 p_{\text{O}_2}^{0.21} \quad 2.7$$

The corresponding empirical relationships between the mole fraction of copper oxide and oxygen pressure were;

$$\log N_{\text{Cu}_2\text{O}} = 0.2174 \log p_{\text{O}_2} - 0.0176 \text{ (Mihalop)} \quad 2.8$$

$$\log N_{\text{Cu}_2\text{O}} = 0.22 \log p_{\text{O}_2} - 0.05 \text{ (Ruddle et al)} \quad 2.9$$

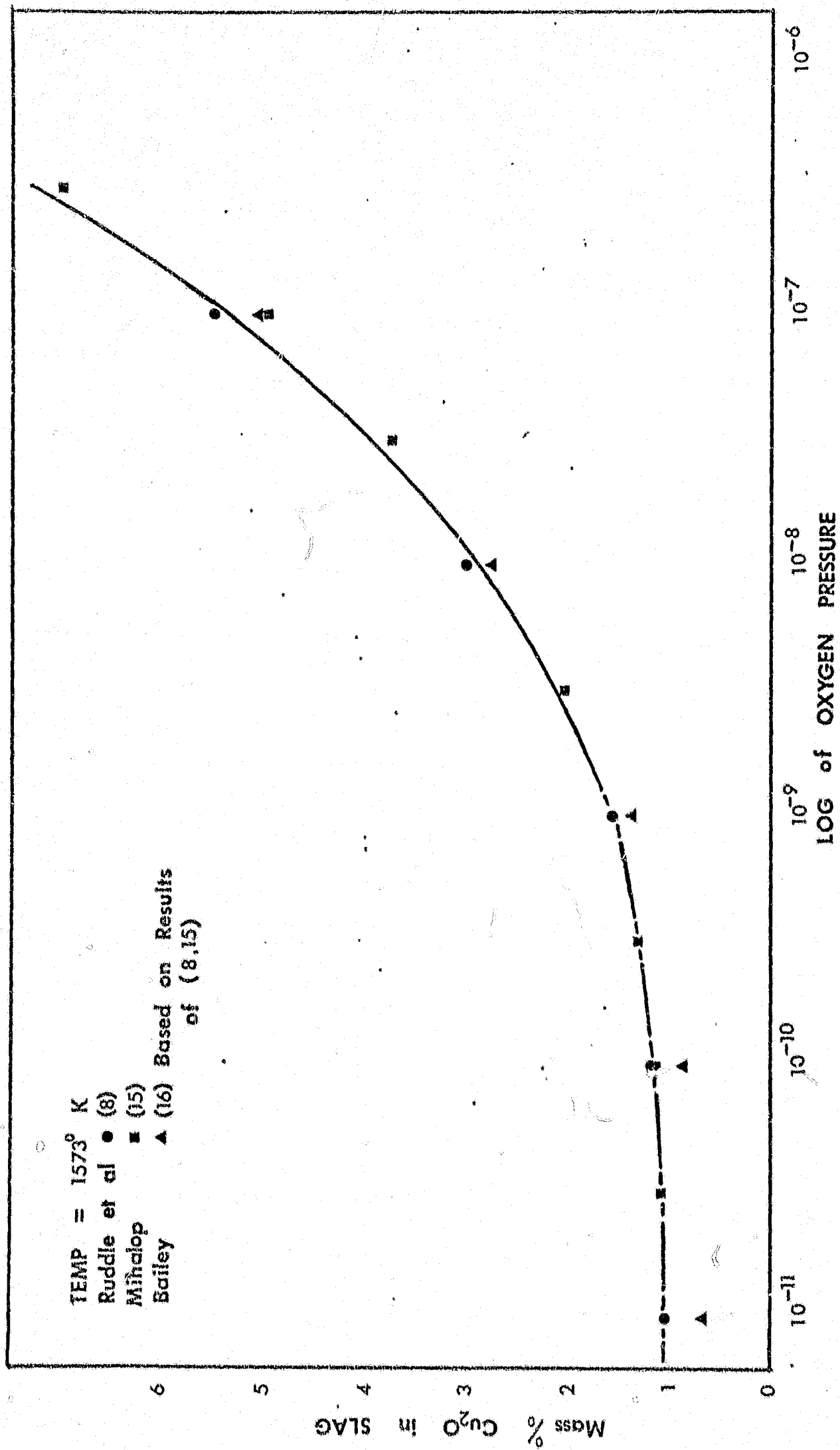


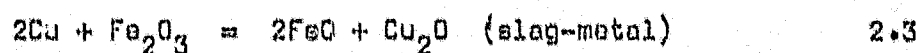
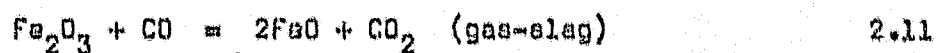
FIGURE 1. COPPER OXIDE in SLAG VERSUS OXYGEN PARTIAL PRESSURE for SILICA - SATURATED IRON SILICATE SLAGS

Bailey (16) investigated the equilibrium between liquid copper and silica-saturated iron silicate slag to resolve the discrepancies between the results of Ruddle et al and Mihalop. The results of all three investigations are presented in Figure 1. Bailey concentrated on the extreme values of oxygen partial pressure and found initially that his values were considerably lower than those obtained in the other two investigations. Between the extremes all three sets of results were in close agreement. Bailey argued that his lower values of copper solubility at higher oxygen partial pressures were a result of the non-attainment of equilibrium and occurred because of the degree of oxidation of the slag which had a high initial ferric iron content. Indeed a longer equilibration time gave higher values of copper solubility which were in close agreement with the results of Mihalop.

Toguri and Santander (17, 20) used copper-gold alloys and a similar technique to that of Ruddle et al except that the alloy-iron silicate slag system was contained in alumina crucibles. The effects of oxygen partial pressure, temperature and the activity of copper in the alloy on the solubility of copper in the slag were determined. The results showed that the copper content of the slag was proportional to the activity of copper in the alloy and the fourth root of the partial pressure of oxygen above the melt.

$$16 \text{ (mass per cent Cu in slag)} = \text{CONSTANT } a_{\text{Cu}}^{1/4} p_{\text{O}_2}^{1/4} \quad 2.10$$

Toguri and Santander discussed their results in terms of the equilibrium reactions between the gas, slag and metal phases.



for which

$$K_3 = \frac{K_{11}}{K_{12}} \frac{a_{\text{Cu}_2\text{O}}}{a_{\text{Cu}}^2 P_{\text{O}_2}^{1/2}} \quad 2.13$$

From Temkin's model

$$a_{\text{Cu}_2\text{O}} = (N_{\text{Cu}^+}^2)(N_{\text{O}^{2-}})(\gamma_{\text{Cu}_2\text{O}}) \quad 2.14$$

using the assumptions that  $N_{\text{O}^{2-}}$  is approximately constant and the solution is dilute. Thus the activity of cuprous oxide is proportional to the mass per cent copper in the slag.

$$\text{ie } a_{\text{Cu}_2\text{O}} \propto (\text{mass \% Cu in slag})^2 \quad 2.15$$

and

$$(\text{mass \% Cu in slag}) \propto \sqrt{\frac{K_3 K_{12}}{K_{11}}} a_{\text{Cu}} P_{\text{O}_2}^{1/2} \quad 2.16$$

As shown in Figure 2, there was a positive deviation from the linear dependence predicted from the above equation at high partial pressures of oxygen and at copper activities above 0,8 in the alloy. The high values are thought to be due to local precipitation of copper as discussed by Richardson and Sillington (21). Employing the least squares technique for analysis of their data, Toguri and Santander obtained the expression

$$\text{mass \% Cu in slag} = 29,73 a_{\text{Cu}_2\text{O}}^{1/2} \quad 2.17$$

Altman and Kellogg (10) obtained results for copper solubility in silica-saturated slags that support a model in which copper exists in the slag as a mononuclear cuprous species represented as  $\text{CuO}_{0,5}$ . The activity of copper in the copper-gold alloy was held at 0,73 relative to pure liquid copper and the oxygen partial pressure was varied using a  $\text{CO}/\text{CO}_2$  gas mixture which was allowed to come to equilibrium with the slag and alloy. The copper



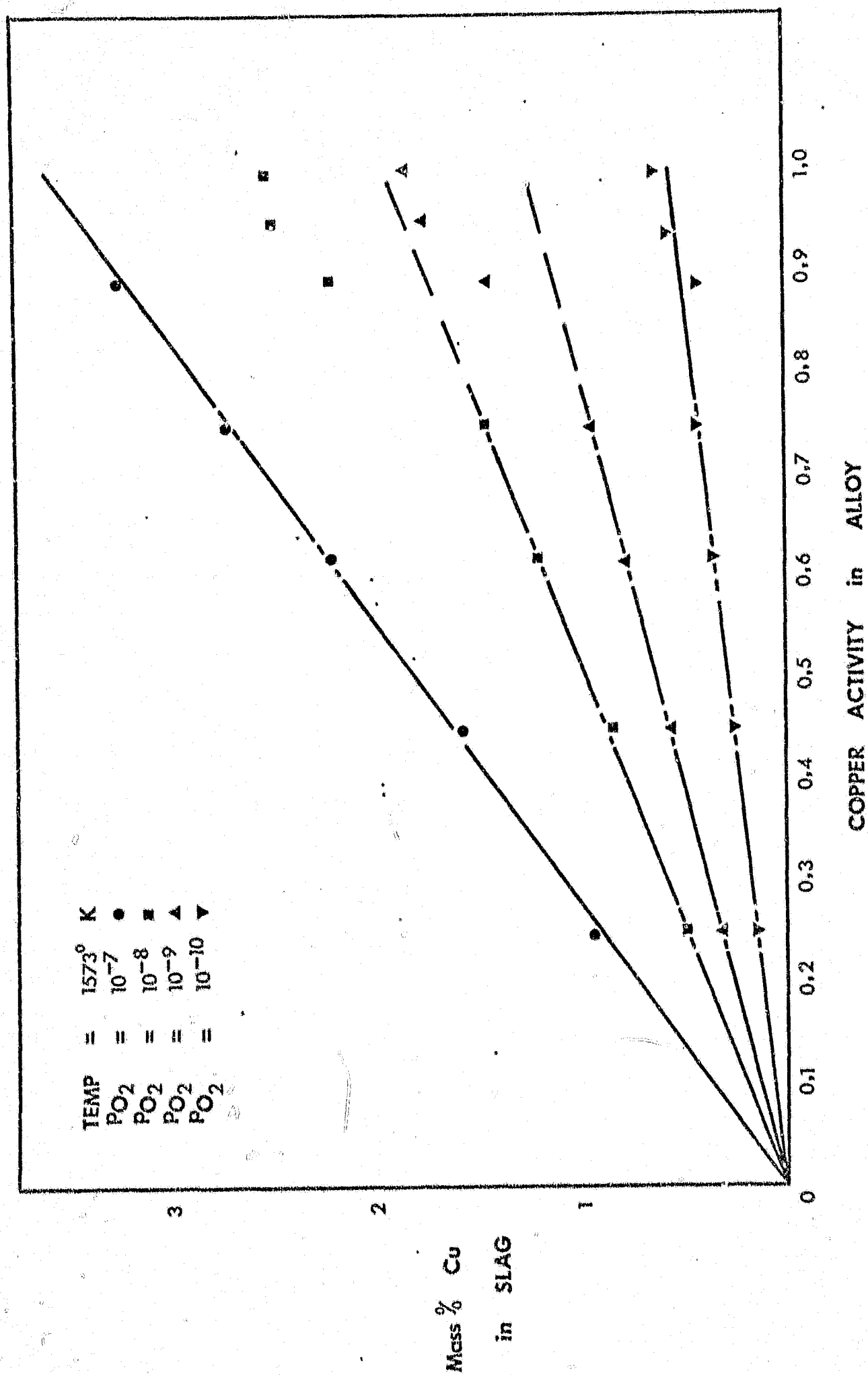


FIGURE 2 RELATION BETWEEN COPPER in SLAG and  
ACTIVITY of COPPER in the ALLOY ( 17 )



solubility data was smoothed for the effect of temperature and slag composition on the activity of  $\text{CuO}_{0.5}$ . Figure 3 shows the activity of  $\text{CuO}_{0.5}$  as a function of the mass per cent copper in the slag. The studies of Taylor and Jaffee (22), Altman and Kellogg (18), Ruddie et al (8) and Toguri and Santander (17) appear to be reasonably consistent up to 4 mass per cent copper in the slag. The results for copper solubility in slag for Bailey (16) are considerably lower and this is probably because the equilibration time was too short.

Altman and Kellogg calculated  $\gamma_{\text{CuO}_{0.5}}$  and found that this activity coefficient exhibited a slight positive deviation from ideal behaviour before reaching a constant value as  $N_{\text{CuO}_{0.5}}$  approached zero and hence in this region the species  $\text{CuO}_{0.5}$  obeyed Henry's law. The species  $\text{Cu}_2\text{O}$  exhibited a strong negative deviation from ideality over the same range of  $N_{\text{Cu}_2\text{O}}$ . The negative deviation might have been the result of complexing of the species  $\text{Cu}_2\text{O}$ . However there is no evidence for the existence of such complexes.

Taylor and Jaffee (22) used the levitation technique to equilibrate copper-gold alloy with silica-saturated slag. This technique can lead to the development of temperature differences between the metal and slag giving incorrect equilibrium data. The results obtained at  $1573^\circ \text{K}$  are compared with those of Ruddie et al, Toguri and Santander and Altman and Kellogg in Figure 3. The results are in very good agreement with those of Altman and Kellogg. The slightly lower solubility of copper in the slags of Toguri and Santander might be explained by the presence of alumina in the slag.

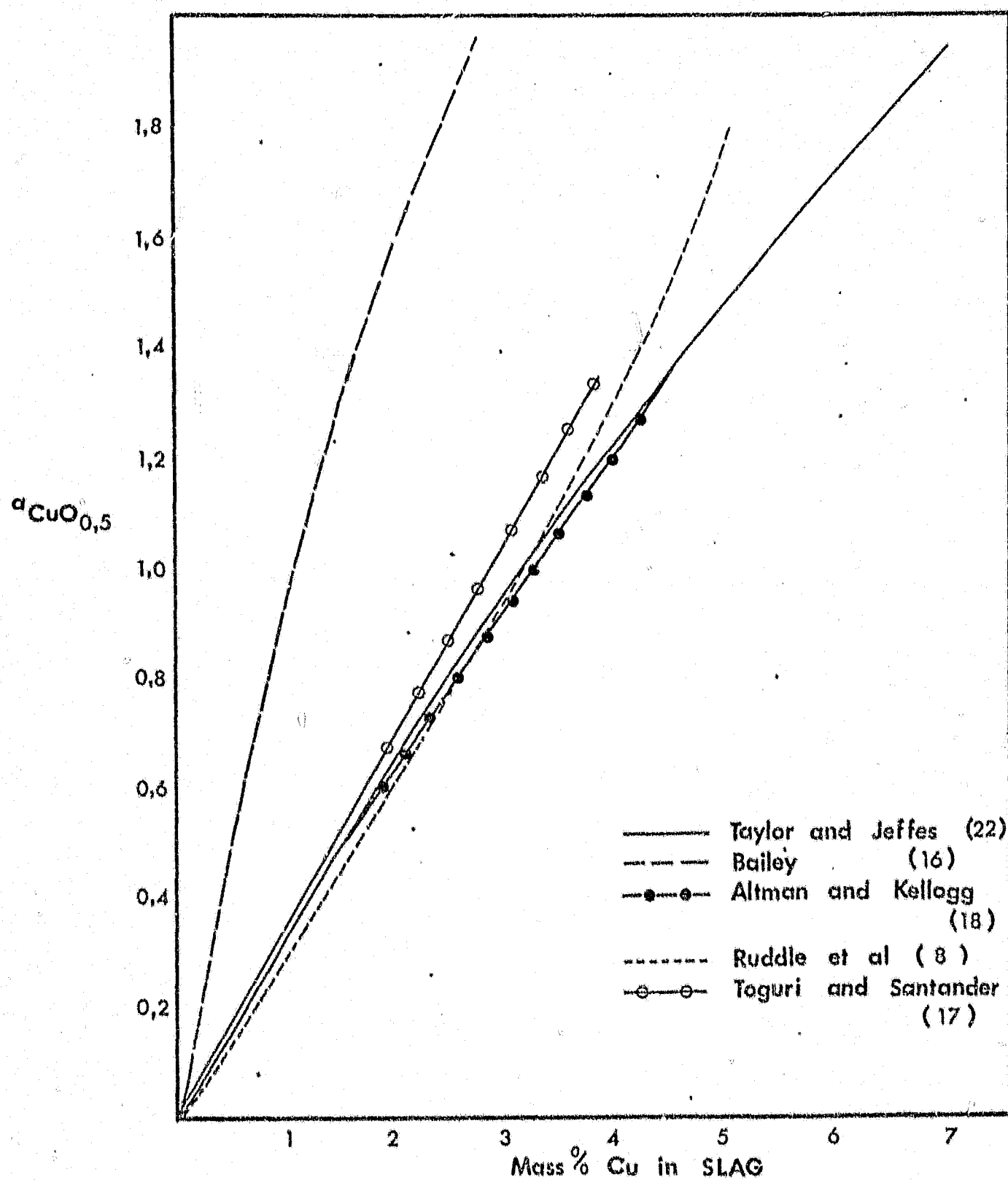


FIGURE 3

COPPER SOLUBILITY in SLAG as a  
FUNCTION of COPPER OXIDE ACTIVITY  
from TAYLOR and JEFFES (22)

### 2.3.2 Temperature

Ruddle et al (8) investigated copper solubility in fayalite slag at temperatures of 1573° K, 1623° K and 1673° K. At a fixed oxygen partial pressure, the copper solubility in the slag and the ferric ion content decreased with increasing temperature. A similar trend was observed by Altman and Kellogg (18) over the temperature range 1500 to 1560° K.

Toguri and Santander (20) investigated the effect of varying temperature from 1523 to 1623° K on the solubility of copper in silica-saturated iron silicate slag for partial pressures of oxygen from  $10^{-7}$  to  $10^{-10}$  atm. The solubility of copper in the slag decreased with increasing temperature, as predicted by the temperature dependence of the equilibrium constant for the reaction



The results are presented in Figure 4 for an oxygen partial pressure of  $10^{-8}$  atm. Taylor and Jeffes (22) also showed that copper solubility decreased with increasing temperature over the temperature range 1573 - 1773° K. Very little effect of temperature on  $\chi_{\text{CuO}_{0.5}}$  was observed for a large variation in slag composition.

### 2.3.3 Slag Composition

The effect of slag composition on copper losses in copper smelting has long been realised. As early as 1912 Wanjukoff (23) studied the effects on slag losses of copper of minor slag constituents such as  $\text{Al}_2\text{O}_3$ ,  $\text{CaO}$  and  $\text{MgO}$ .

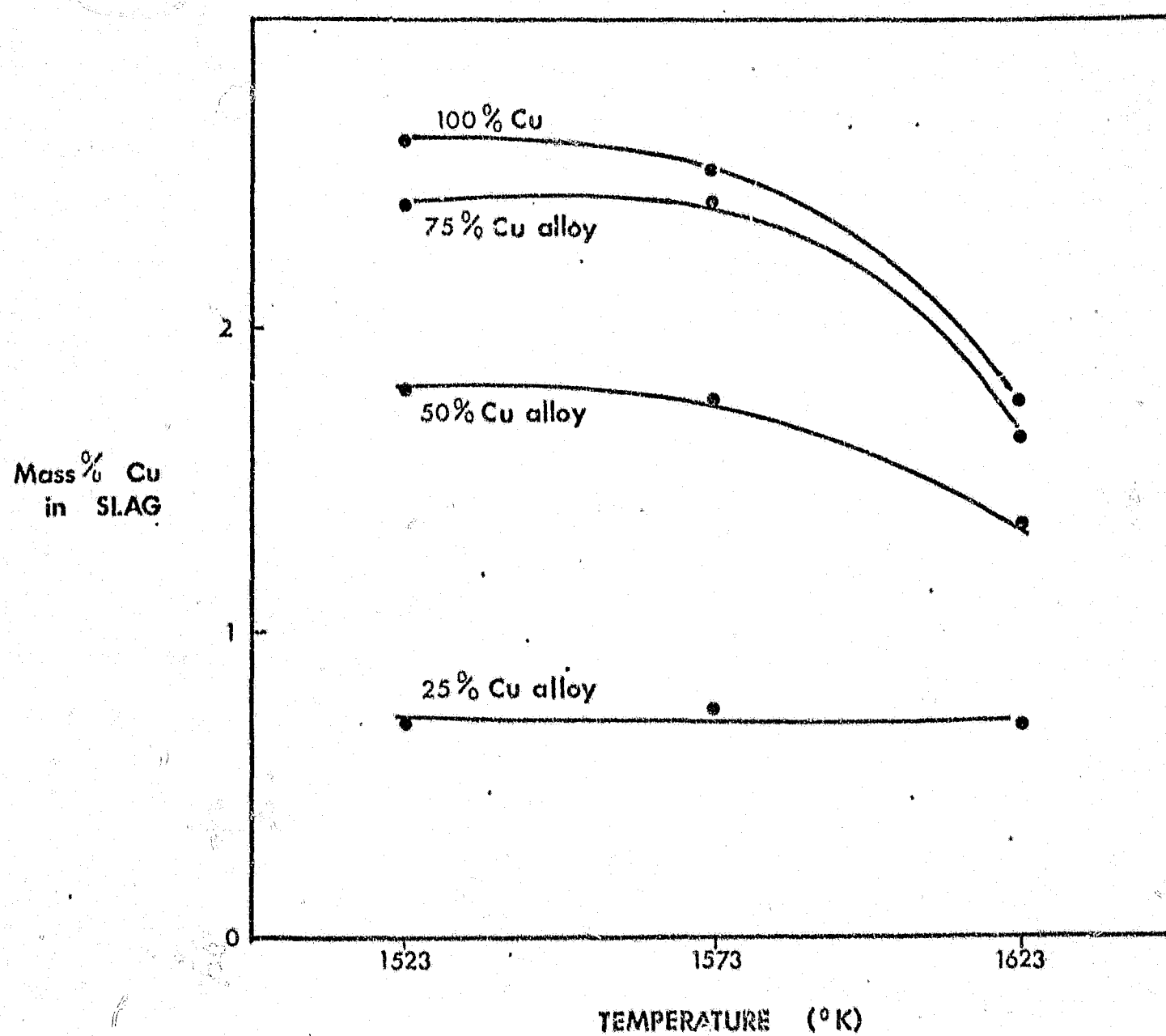


FIGURE 4

EFFECT of TEMPERATURE on the  
 SOLUBILITY of COPPER in SLAG  
 at  $PO_2 = 10^{-8}$  atm from  
 TOGURI and SANTANDER (20)

### 2.3.3.1 Iron

Bailey et al (24) noticed a considerable difference between the iron content of an equilibrated Rokana slag and synthetic slag. A curve of  $(\% \text{Cu}_2\text{O})/(\% \text{Fe})$  in slag verses  $\log p_{\text{O}_2}$  (Figure 5.) showed that the copper solubility at a particular oxygen partial pressure was directly related to its iron content. Furthermore the minor slag components did not significantly alter this relationship.

For experiments on iron silicate slags with a high iron content the only suitable crucible material is alumina. Bailey (16) first evaluated the effect of alumina on copper solubility. The solubility of alumina varied from 16 mass per cent for slags containing 45 mass per cent iron to 4 mass per cent alumina at saturation for slags containing 56 mass per cent iron.

Bailey observed that the copper contents of the slags increased in the order high-iron, medium-iron and silica-saturated slags as shown in Figure 6. If the effect of alumina is considered the solubility of copper in slag is lowered if the iron content is increased above 40 mass per cent. This result conflicts with the prediction from the curve in Figure 5.

Taylor and Jeffes (22) investigated the variation in copper solubility in iron silicate slags of varying composition and observed that  $a_{\text{Cu}_2\text{O},5}$  decreased as  $a_{\text{FeO}}$  increased. It was considered that this was because of the difference in the relative stabilities of copper silicates and ferrites.

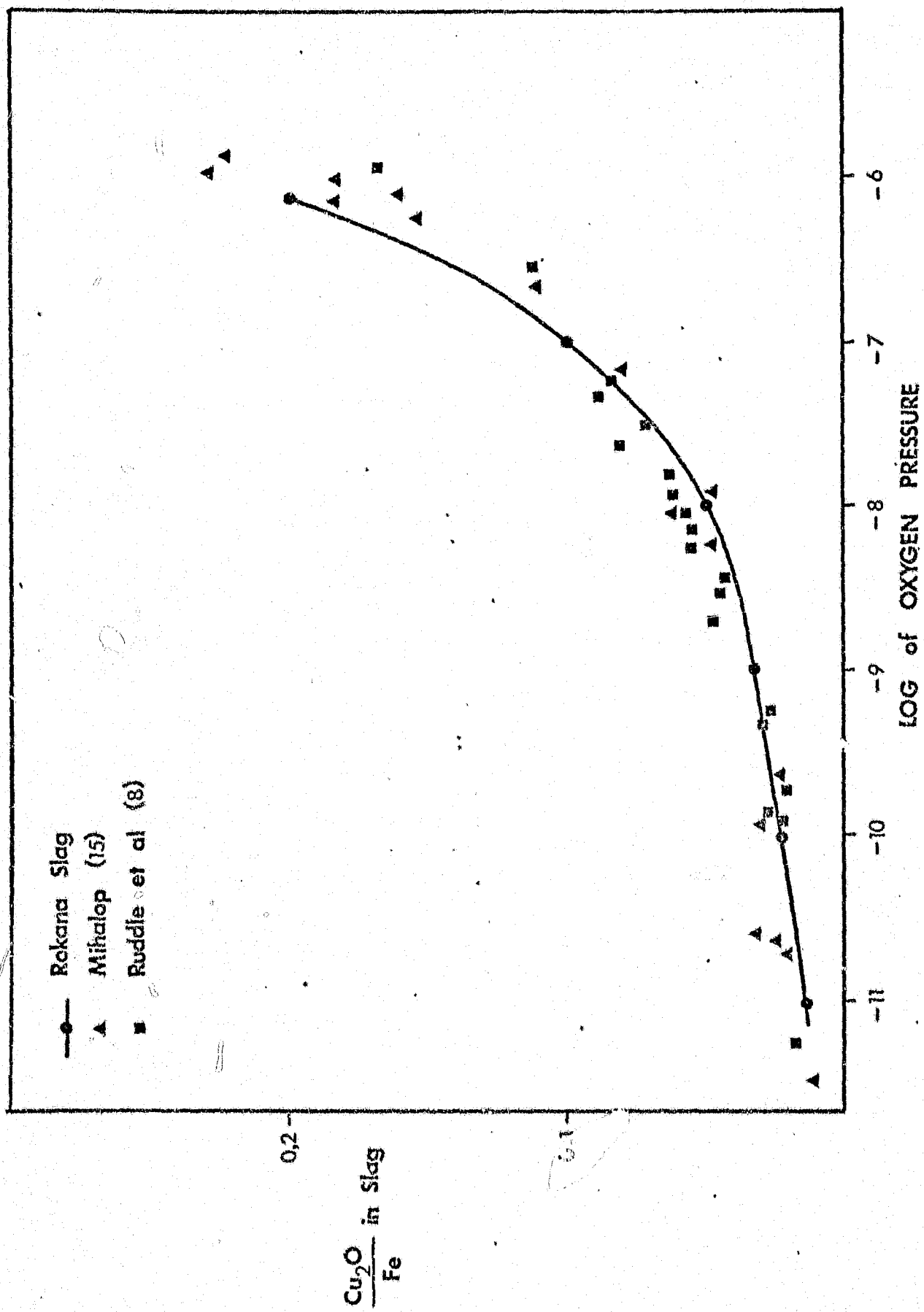


FIGURE 5  
RATIO of COPPER to IRON in SLAG VERSUS  
PARTIAL PRESSURE of OXYGEN at 1573° K (16)

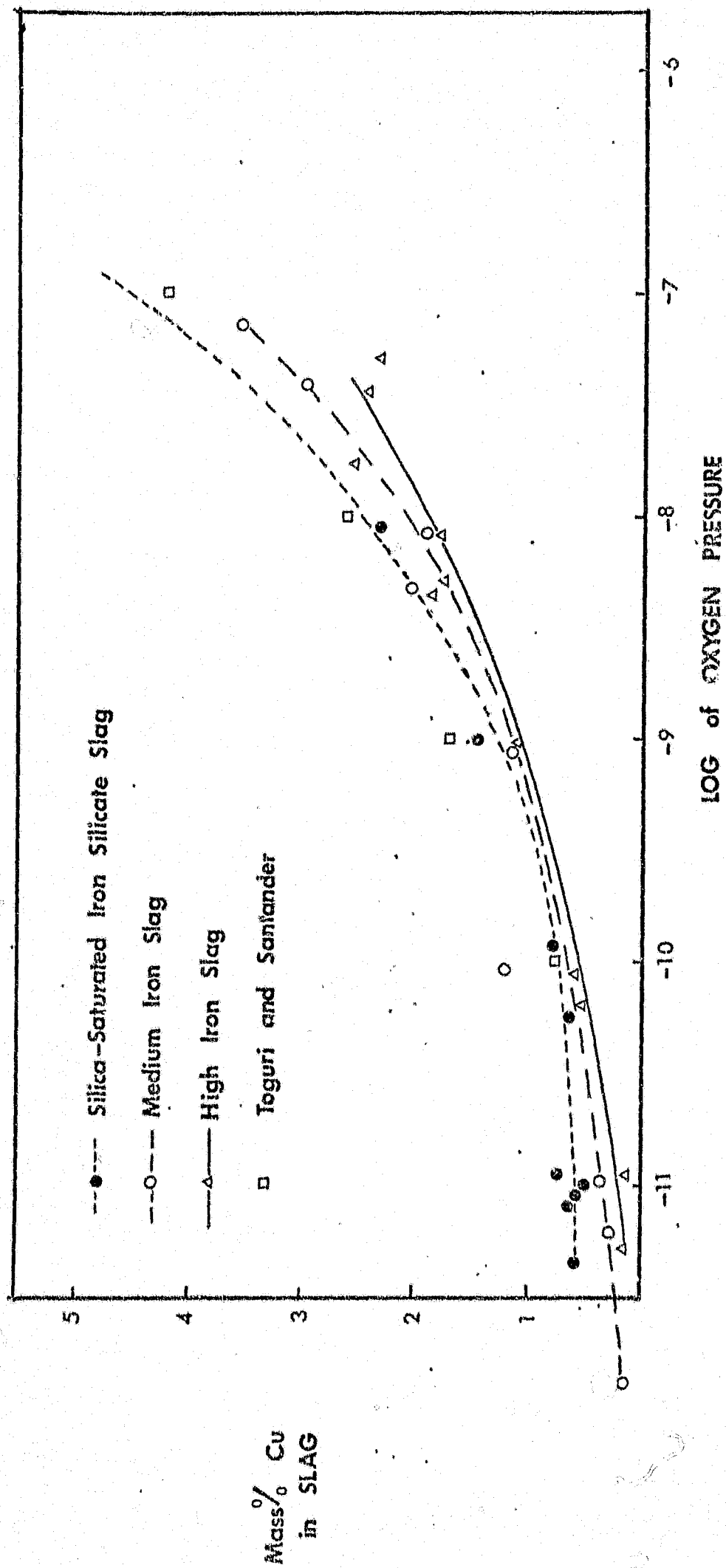


FIGURE 6 COPPER in the SLAG VERSUS OXYGEN PARTIAL PRESSURE for HIGHER IRON SLAGS from BAILEY (16)

### 2.3.3.2 Alumina

The first comprehensive paper on the relationships between slag composition and slag copper content was published by Wanjukoff (23) in 1912. The charge contained matte assaying 30 mass per cent copper and was melted in a graphite crucible for  $1\frac{1}{2}$  hours and allowed to cool inside the furnace. Premixing of the charge components might have increased the possibility of entrainment of copper into the slag and the equilibration time of  $1\frac{1}{2}$  hours appears to have been insufficient for equilibrium to be reached. Slow cooling of the sample may also have caused some copper to precipitate, from the slag before it had solidified.

Wanjukoff's results indicated that alumina acted as a diluent. Replacement of lime with alumina produced inconclusive results as the copper solubility initially decreased by as much as 10 per cent of its original value but then increased to its original value for alumina additions between 10 to 25 mass per cent.

Investigations by Scobie (25) and Ruddle et al (8) also produced inconclusive results. Scobie mixed the charge material and heated it in a fireclay crucible in an electric furnace. The charge was held at  $1643^{\circ}$  K for one hour and then cooled to room temperature. Reducing conditions were maintained by additions of powdered coal to the charge. However, due to scatter in the results no definite conclusions can be made.

Scobie explained the effect of slag composition by suggesting that the amount of copper in the slag could be represented by the



the following equation.

$$Cu_s = (SD \times fSD) + (\%Al_2O_3 \times fAl_2O_3) + (\%CaO \times fCaO) + (\%MgO \times fMgO) \quad 2.18$$

where  $Cu_s$  = Copper in the slag

$SD$  = Silicate degree =  $\frac{\text{oxygen combined with silica}}{\text{oxygen combined with iron}}$

$fSD, fAl_2O_3$  etc = silicate degree factor, alumina degree factor etc

However, the data failed to support the equation.

Ruddle et al (8) performed a series of experiments to study the effect of small additions of  $Al_2O_3$ ,  $MgO$ ,  $CaO$  and  $ZnO$  on copper solubility in the slag. The silica-saturated iron silicate slags were brought to equilibrium with pure copper at  $1573^\circ K$ . No significant variations in the copper content of the slag were observed.

Toguri and Santander (17) used alumina crucibles in their experiments to establish the effect of the partial pressure of oxygen on the solubility of copper in iron silicate slags. The solubility of copper was slightly lower than the values obtained by Ruddle et al (8) and Altman and Kellogg (18) for silica-saturated slags without alumina. This difference was attributed to the presence of alumina ( $6.0 \pm 0.5$  mass per cent) in the slag. These three investigations are compared in Figure 3.

Nagamori, Mackay and Tarasoff (26) equilibrated pure copper with silica-unsaturated fayalite slags in alumina crucibles. The slags contained an average of 8 mass per cent  $Al_2O_3$  over the range of partial pressures of oxygen from  $10^{-6}$  to  $10^{-11}$  atm. Nagamori et al concluded that the presence of  $Al_2O_3$  lowers the copper solubility.

In a more extensive study, Bailey and Garner (16, 27) equilibrated 5 g of pure copper with 20 g of fayalite slag containing either 5 or 10 mass per cent alumina. Figure 7 shows that there is little difference in the solubility of copper between alumina-free slag and slag containing 5 mass per cent alumina. The slight difference was attributed to the reduction in the iron content of the slag from 44 mass per cent to 38 mass per cent. For additions of up to 5 mass per cent, alumina did not affect the solubility of copper. For slag containing 10 mass per cent alumina there was a significant increase in the solubility of copper. These results indicate that the effect of alumina is dependent on its concentration. It appears that for a particular slag there is a critical alumina concentration above which there is a marked effect on the copper solubility.

#### 2.3.3.3 Magnesia

Due to scatter no conclusive results have been obtained for the effect of magnesia on copper solubility by Wanjukoff (23), Seobie (25) and Ruddle et al (8). However, it is generally felt that as much as 8 mass per cent magnesia does not significantly alter the solubility of copper in slag.

#### 2.3.3.4 Lime

There is general agreement that the solubility of copper in slag is reduced with increasing CaO content of the slag (1, 2, 8, 10, 28). Montil'o et al (28) studied a matte-silicate slag system for

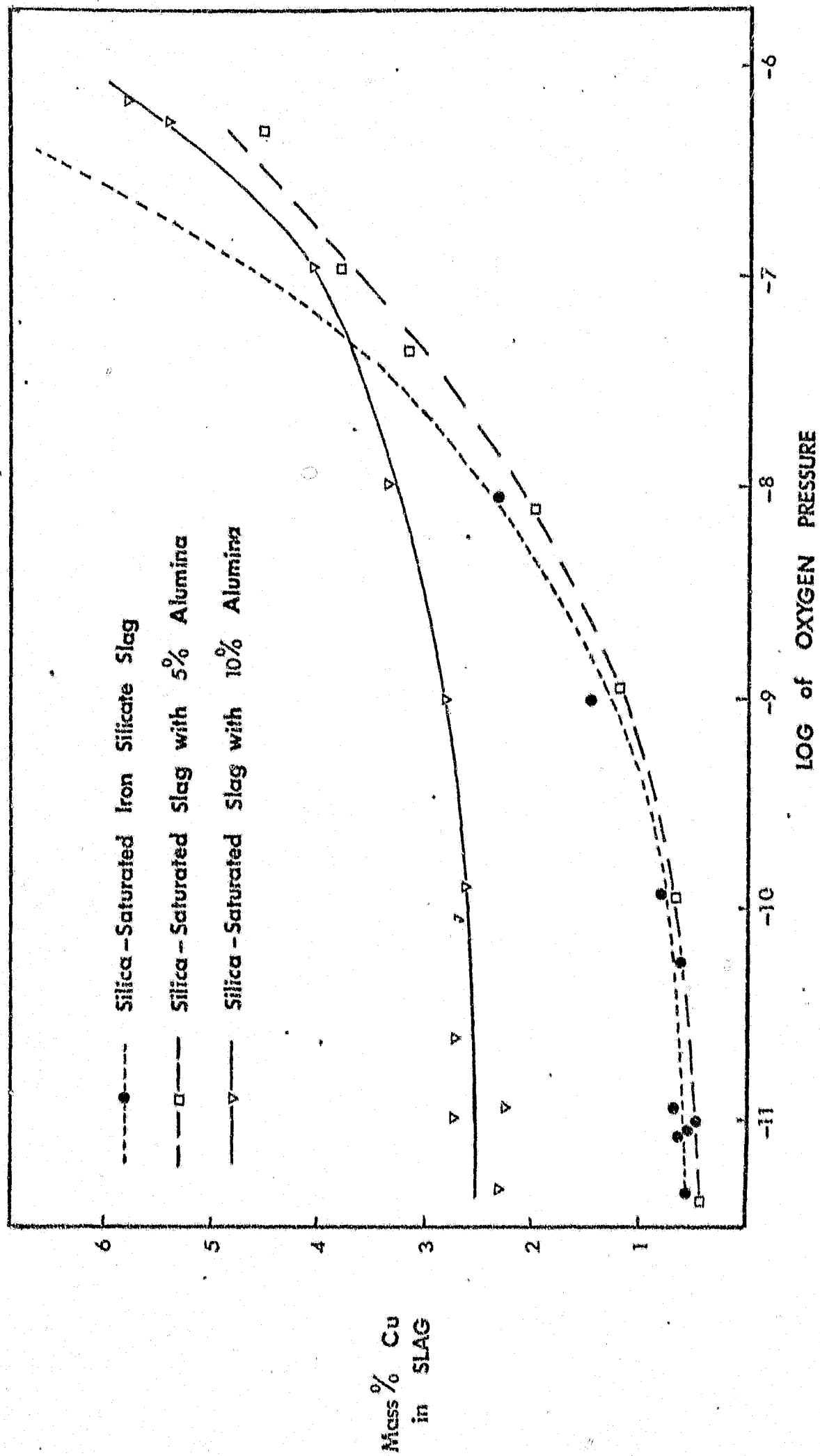


FIGURE 7 COPPER in the SLAG VERSUS OXYGEN PARTIAL PRESSURE for  
SILICA-SATURATED SLAGS from BAILEY (16)

lime contents in the slag of between 6 to 8 mass per cent and observed a reduction in the dissolved copper content. This is thought to be due to the relative basicities of copper oxide and lime. The silica content of the slag varied from between 20 to 30 mass per cent.

#### 2.3.4 Summary and Comparison of Different Investigations

Previous work indicates that the solubility of copper in silica-saturated iron silicate slag depends upon the partial pressure of oxygen above the melt, the temperature and the composition of the slag.

The solubility of copper in slag increases with increasing partial pressure of oxygen between the limits of iron saturation and magnetite saturation, whilst an increase in slag temperature decreases the solubility of copper in the slag.

At a particular partial pressure of oxygen an increase in the iron content of the slag produces a decrease in the solubility of copper in the slag. From the work of Bailey (16) the effect of alumina on copper solubility appears to be dependent on its concentration in the slag. At a partial pressure of oxygen of  $10^{-8}$  atm the addition of 5 mass per cent  $Al_2O_3$  lowers the solubility of copper in slag whilst the addition of 10 mass per cent  $Al_2O_3$  increases the solubility of copper in the slag (Figure 7). The results for 10 mass per cent  $Al_2O_3$  appear to be in error as discussed later (Section 5.2.2).

TABLE 2.1 SUMMARY OF INVESTIGATIONS ON COPPER SOLUBILITY IN SLAG

PARAMETER	SLAG	ALLOY	INVESTIGATOR	RESULT (Expressed as mass % Cu in slag)
Partial pressure of oxygen	Silica-saturated	Pure Cu	Ruddle et al (8)	33,64 <sup>a</sup> CuO <sub>0,5</sub>
	Silica-saturated	Pure Cu	Mihalop (15)	35,69 <sup>a</sup> CuO <sub>0,5</sub>
	Iron-silicate slag containing Al <sub>2</sub> O <sub>3</sub>	Cu-Au Alloy	Toguri and Santander (17)	29,73 <sup>a</sup> CuO <sub>0,5</sub>
	Silica-saturated	Cu-Au Alloy	Altman and Kellogg (18)	35,69 <sup>a</sup> CuO <sub>0,5</sub>
	High-silica	Cu-Au Alloy	Taylor and Jeffes (22)	32,45 <sup>a</sup> CuO <sub>0,5</sub>

TABLE 2.1 cont. SUMMARY OF INVESTIGATIONS ON COPPER SOLUBILITY IN SLAG

PARAMETER	SLAG	ALLOY	INVESTIGATOR	RESULT (Expressed as mass % Cu in slag)
Temperature	Iron-silicate slag containing $Al_2O_3$	Cu-Au Alloy	Toguri and Santander (20) (at 1523° K) (at 1573° K) (at 1623° K)	27,59 <sup>a</sup> CuO <sub>0,5</sub> 29,44 <sup>a</sup> CuO <sub>0,5</sub> 30,57 <sup>a</sup> CuO <sub>0,5</sub>
Iron	Iron-silicate	Pure Cu	Bailey (16) Medium Iron High Iron	27,26 <sup>a</sup> CuO <sub>0,5</sub> 24,66 <sup>a</sup> CuO <sub>0,5</sub>
Alumina	Silica-saturated	Pure Cu	Bailey (16) 5 mass % $Al_2O_3$ 10 mass % $Al_2O_3$	27,52 <sup>a</sup> CuO <sub>0,5</sub> 42,45 <sup>a</sup> CuO <sub>0,5</sub>

The effects of these parameters on the solubility of copper in slag are summarized in Table 2.1. The results are presented as mass per cent copper in the slag related to the activity of copper oxide in the form  $\text{CuO}_{0.5}$  in the slag.

Each result in Table 2.1 has been calculated from the raw experimental copper solubility data of the respective investigations at a partial pressure of oxygen of  $10^{-8}$  atm. For copper equilibrated with silica-saturated iron silicate slag the results of Ruddle et al (8), Mihalop (15) and Altman and Kellogg (18) are in good agreement. The result for Taylor and Jeffes (22) is slightly lower and could be the result of the difficulties experienced in temperature control, using the levitation technique. Toguri and Santander's (17) results are lower due to the alumina content of the slag and the probability that the slags were not silica-saturated.

### 3. EXPERIMENTAL

The solubility of copper in silica-saturated slag was studied by equilibrating a copper-gold alloy with an iron silicate slag in silica crucibles at  $1573^{\circ}$  K under a known oxygen partial pressure of  $8 \times 10^{-9}$  atm maintained by a CO/CO<sub>2</sub> gas mixture. The activity of copper in the copper-gold alloy was varied from 0,3 to 1,0 relative to pure liquid copper as the standard state and the effect of additions of MgO, Al<sub>2</sub>O<sub>3</sub> and CaO on the solubility of copper was examined.

#### 3.1 Experimental Design

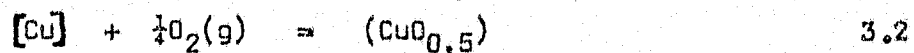
The experimental programme was designed to determine the solubility of copper when copper-gold alloys are equilibrated with silica-saturated iron silicate slag. The advantage in using a copper-gold alloy is that it is then possible to vary the activity of copper in the alloy and thus the activity of copper oxide in the slag

$$\text{is } a_{\text{CuO},5} \propto a_{\text{Cu}^0\text{O}_2}^{\frac{1}{2}} \quad 3.1$$

The additional advantage in using gold in the alloy is to establish the extent to which copper is entrained in the slag from the analytical value of gold content in the slag. Gold exhibits a solubility of 0,008 mass per cent (18) at  $1573^{\circ}$  K relative to pure gold and values obtained for the gold content of the slag can be seen in Figure 19.



The solution of copper in slag is represented by the simple oxidation reaction



The reasons for the choice of  $\text{CuO}_{0,5}$  as the copper molecular species are discussed later.

For the four phase system shown below,

$\text{O}_2$	GAS
$\text{SiO}_2\text{-FeO-Fe}_2\text{O}_3\text{-CuO}_{0,5}$	SLAG
$\text{Fe-Cu-Au}$	ALLOY
$\text{SiO}_2$	CRUCIBLE

there are 5 components; ie, all other species in the system may be formed from a minimum of 5 species. These may be considered as Cu, Au, Si, Fe and  $\text{O}_2$ . From the phase rule,

$$F = C + 2 - P \quad 3.3$$

where C is the number of components, P is the number of phases and F is the number of degrees of freedom,

$$F = 5 + 2 - 4 = 3$$

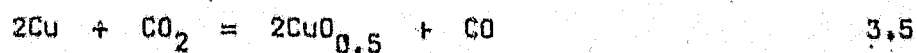
This means that in order to have unique values of any parameter three variables must be held constant. Experimentally, temperature and partial pressure of oxygen are easily controlled. Therefore at constant temperature and partial pressure of oxygen unique values of  $N_{\text{CuO}_{0,5}}$  are obtained at each concentration of copper in the alloy. Copper concentration in the alloy may be varied by dilution of copper with inert gold. From equation 3.1 it can be seen that at any fixed partial pressure of oxygen a range of  $\text{CuO}_{0,5}$  values can be obtained over a range of copper contents of the alloy.

In this study 2 g of copper-gold alloy were equilibrated in silica crucibles with 5 g of iron silicate slag. The oxygen partial pressure was fixed by the equilibrium attained in a mixture of carbon dioxide and carbon monoxide



The partial pressure of oxygen for reverberatory smelting is commonly in the region of  $10^{-10}$  atm and for converting in the region of  $10^{-8}$  atm (26). Continuous smelting and converting processes operate over the range of oxygen partial pressure  $10^{-5}$  to  $10^{-7}$  atm whilst flash, blast and slag reduction furnaces operate in the region  $10^{-10}$  to  $10^{-11}$  atm (26). The oxygen partial pressure of  $8 \times 10^{-9}$  atm used in this investigation is more representative of converter smelting.

Equations 3.2 and 3.4 may be combined to give the equilibrium reaction



for which the equilibrium constant K is

$$K = \frac{a_{\text{CuO}_{0.5}}^2}{a_{\text{Cu}}^2} \frac{P_{\text{CO}}}{P_{\text{CO}_2}} \quad 3.6$$

$$\text{thus } a_{\text{CuO}_{0.5}} = \sqrt{K \frac{P_{\text{CO}}}{P_{\text{CO}_2}}} a_{\text{Cu}} \quad 3.7$$

$$\text{and } a_{\text{Cu}_{0.5}} = N_{\text{CuO}_{0.5}} X_{\text{CuO}_{0.5}} \quad 3.8$$

Having established this simple relationship the effects on copper solubility in the slag of individual additions of MgO,  $\text{Al}_2\text{O}_3$ , and CaO were investigated under identical conditions of temperature and partial pressure of oxygen. The addition of one of the fluxing

components  $\text{MgO}$ ,  $\text{Al}_2\text{O}_3$  or  $\text{CaO}$  to the above system increases the number of degrees of freedom to a total of 4. Therefore, a further variable such as the concentration of  $\text{MgO}$ ,  $\text{Al}_2\text{O}_3$  or  $\text{CaO}$  must be controlled. At a temperature of  $1573^\circ\text{K}$  and an oxygen partial pressure of  $8 \times 10^{-9}$  atm oxygen the slag composition was varied by the addition of up to 4 mass per cent  $\text{MgO}$ , 8 mass per cent  $\text{Al}_2\text{O}_3$  and 10,5 mass per cent  $\text{CaO}$ .

### 3.2 Basic Experimental Procedure

The initial charge consisted of 2 g of copper-gold alloy and 5 g of iron silicate slag containing 36,1 mass per cent  $\text{SiO}_2$ , 49,4 mass per cent total iron, and 49,2 mass per cent ferrous iron (Section 3.3.2). The charge was contained in a 10 ml crucible and upon melting the slag phase completely covered the metal phase.

Equilibration of this system at  $1573^\circ\text{K}$  results in the partial reduction of iron oxide in the slag with the subsequent formation of a Cu-Au-Fe alloy. The initial oxygen potential of the slag, defined by the  $\text{Fe}^{3+}/\text{Fe}^{2+}$  ratio at  $1573^\circ\text{K}$ , was kept well below that at  $8 \times 10^{-9}$  atm oxygen to ensure representative analyses once equilibrium has been reached. The  $\text{Fe}^{3+}/\text{Fe}^{2+}$  ratio of the standard slag was 0,004 which was well below the value of 0,090 in slag at equilibrium with an oxygen potential of  $10^{-8}$  atm, and with a silica content of 36,1 mass per cent (19). Values of  $\text{Fe}^{3+}/\text{Fe}^{2+} > 0,50$  tend to give erratic results and require extended periods to establish equilibrium (29). An initial high oxygen potential

of the slag would result in a high copper solubility of which a portion would presumably remain as finely dispersed metal droplets from reduced copper oxide, or as soluble copper in the lattice of unreduced magnetite (18) as equilibrium was attained.

The silica content of the starting slag was 36.1 mass per cent which is comparable with the value of 37.0 mass per cent found in silica-saturated slags at 1573° K and a oxygen potential of  $10^{-8}$  atm (19). The high silica content of the starting slag ensured minimal dissolution of the crucible. However, the significant percentage of crucible failures experienced were due to imperfections in the crucibles such as bubbles in the walls rather than to dissolution of the crucible.

The equilibration time was determined by contacting a copper-gold alloy containing 70.94 mass per cent copper with slag at an oxygen potential of  $8 \times 10^{-9}$  atm for periods up to 40 hours. For each run the compositions and amounts of alloy and slag were constant and the activity of copper in the alloy was about 0.82 at the end of the run.

### 3.3 Materials

In this section, the materials and procedures used to prepare the metal, slag and gas phases are described and the choice of a suitable crucible material is discussed.

### 3.3.1 Slag

A silica-saturated iron silicate slag was used in this study. The slag was prepared from ferrous oxalate, iron powder and pure precipitated silica powder. Decomposition of ferrous oxalate at  $1273^{\circ}$  K produced  $\text{Fe}_2\text{O}_3$  powder which was then mixed with the required amount of silica by dry grinding. Iron powder was added to give a mixture of composition 15,5 mass per cent iron powder, 38,7 mass per cent  $\text{SiO}_2$  and 45,8 mass per cent  $\text{Fe}_2\text{O}_3$ . The final powder mixture was mixed by tumbling for 24 hours. On heating this mixture part of the  $\text{Fe}_2\text{O}_3$  is reduced by the Fe and a slag of fayalite composition is formed.

A mild steel pipe with a welded base was used as the melting crucible. To maintain a reducing atmosphere at the slag surface the iron crucible was placed inside a graphite crucible and zirconia bubble was packed between the two crucibles. The crucible assembly was held in a muffle furnace at  $1623^{\circ}$  K for 5 hours. The molten slag was slowly cooled within the furnace, chipped from its iron container and ground to a suitable size in a Siabteknik mill. The resulting slag analysed 36,1 mass per cent  $\text{SiO}_2$  and 49,4 mass per cent total Fe (49,2 mass per cent  $\text{Fe}^{2+}$ ).

The partial liquidus diagram for the system  $\text{FeO-Fe}_2\text{O}_3\text{-SiO}_2$  is represented in Figure 8 and fayalite composition at silica-saturation and  $1573^{\circ}$  K is represented by the line ad (32). Although information is now available for the quaternary  $\text{Cu-Fe-O-SiO}_2$  (33), the ternary is quite adequate for this investigation.

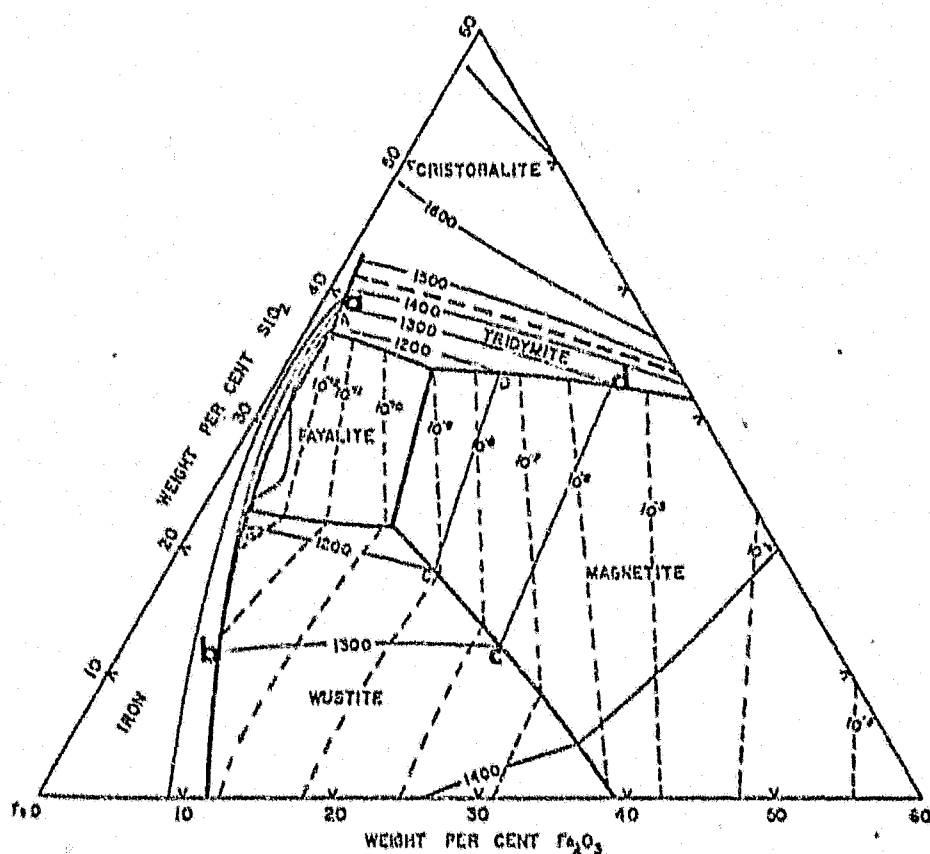


FIGURE 8

PARTIAL LIQUIDUS DIAGRAM for the SYSTEM  
 $\text{FeO}-\text{Fe}_2\text{O}_3-\text{SiO}_2$ . Dotted lines are oxygen isobars (32)  
 from TOGURI, THEMELIS, and JENNINGS (14)

The solubility limits of  $\text{MgO}$ ,  $\text{Al}_2\text{O}_3$  and  $\text{CaO}$  can be evaluated from the ternary diagrams for the systems  $\text{MgO}$ - $\text{FeO}$ - $\text{SiO}_2$ ,  $\text{FeO}$ - $\text{Al}_2\text{O}_3$ - $\text{SiO}_2$  and  $\text{CaO}$ - $\text{FeO}$ - $\text{SiO}_2$  shown in Figures 9, 10 and 11. These diagrams are not entirely satisfactory as they do not include the ferric ion content and thus correspond to the lowest oxidation states. From the Figures the limits of component solubilities at  $1573^\circ \text{K}$  are:

$\text{MgO}$	5 mass per cent
$\text{Al}_2\text{O}_3$	13 mass per cent
$\text{CaO}$	25 mass per cent

In this work values lower than these were used to ensure total solution of  $\text{MgO}$ ,  $\text{CaO}$  and  $\text{Al}_2\text{O}_3$  in the slag.

### 3.3.2 Alloy

The variation in the activities of gold and copper in liquid solutions of  $\text{Cu-Au}$  are shown in Figure 12. The average iron content of the alloy throughout the experimental campaign was less than 0.10 mass per cent and thus its effect on the activity of copper in the alloy was assumed to be negligible. The temperatures of the liquidus lines for the binary alloy are all well below  $1573^\circ \text{K}$  and thus the activity of copper could be varied over the complete composition range of the alloy.

The copper-gold alloys were prepared from mint gold wire (99.99 per cent purity) and electrolytic copper (99.95 per cent purity). The gold wire was cut down, the copper turned on a lathe

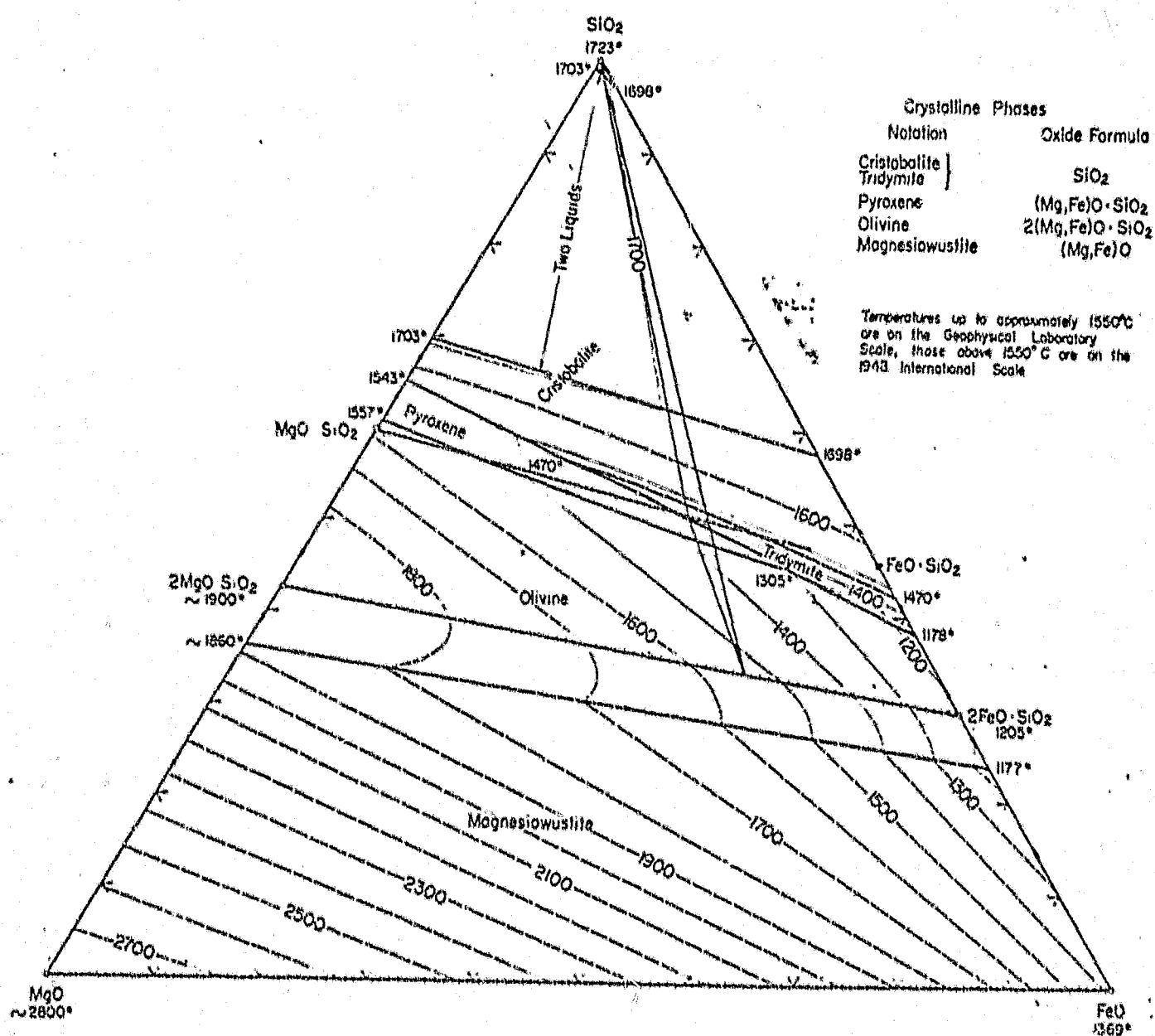


FIGURE 9

LIQUIDUS DIAGRAM for the SYSTEM  
 $\text{MgO} - \text{"FeO"} - \text{SiO}_2$  (31)



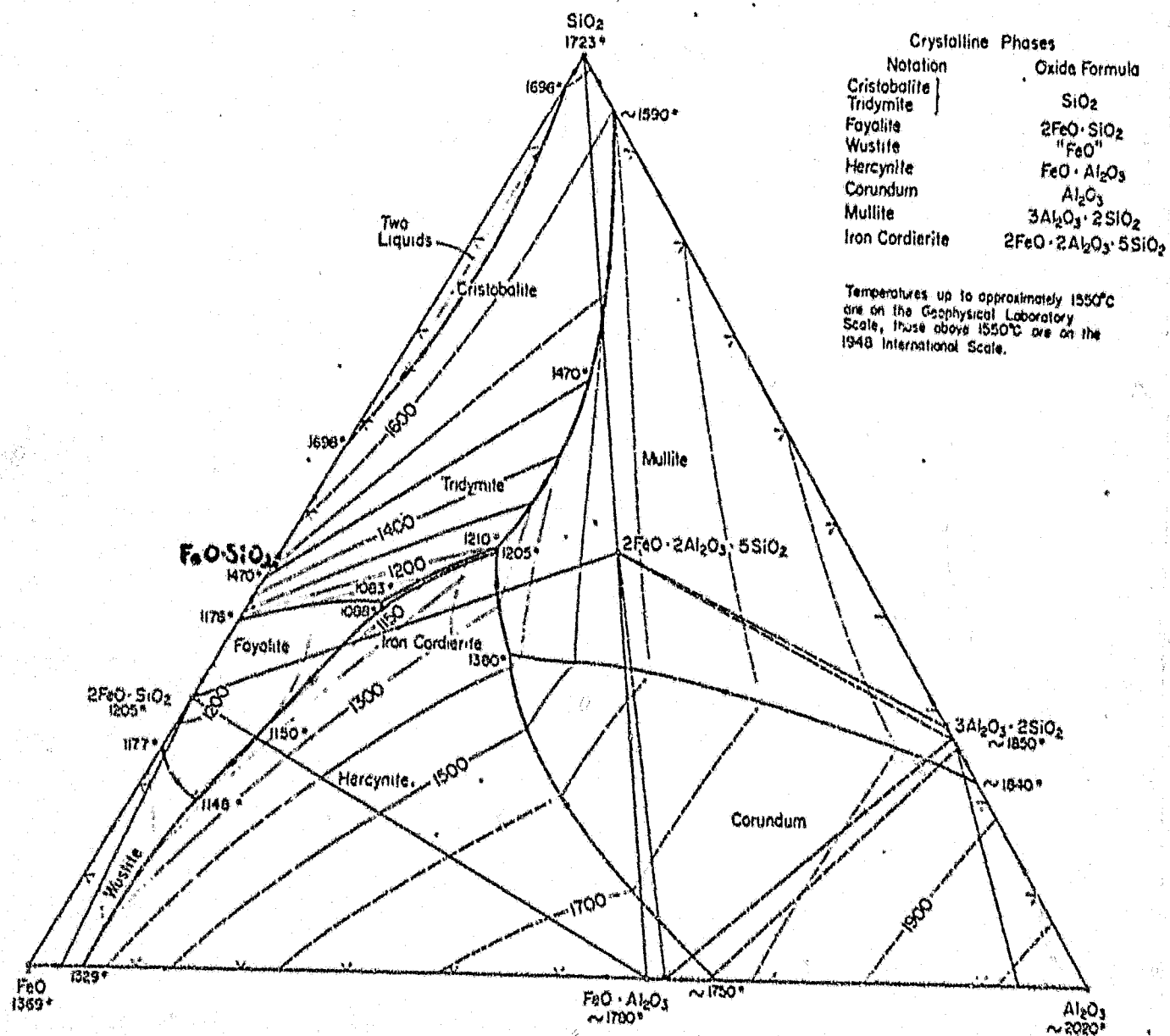
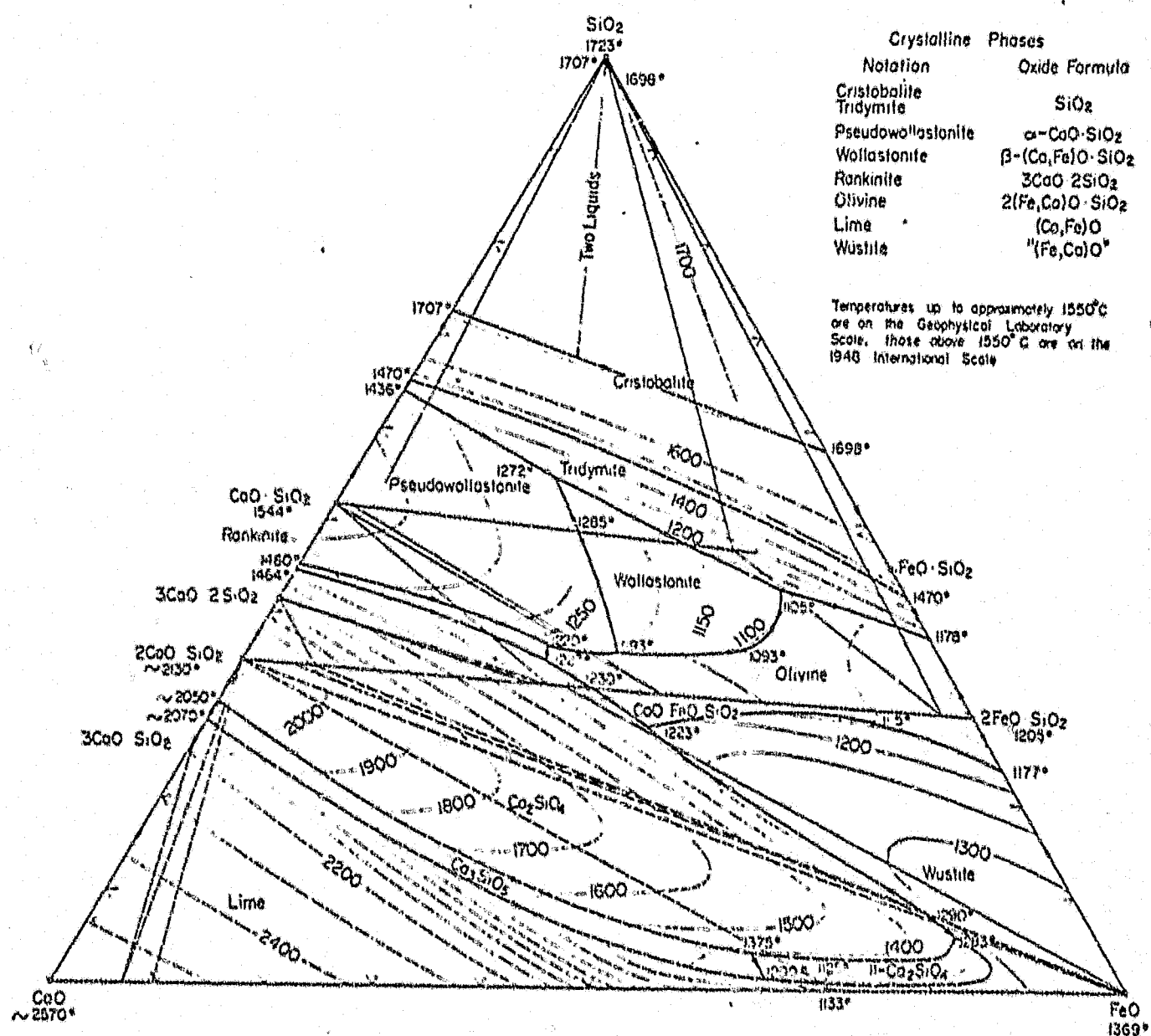


FIGURE 10

LIQUIDUS DIAGRAM for the SYSTEM  
 "FeO" -  $\text{Al}_2\text{O}_3$  -  $\text{SiO}_2$  (31)



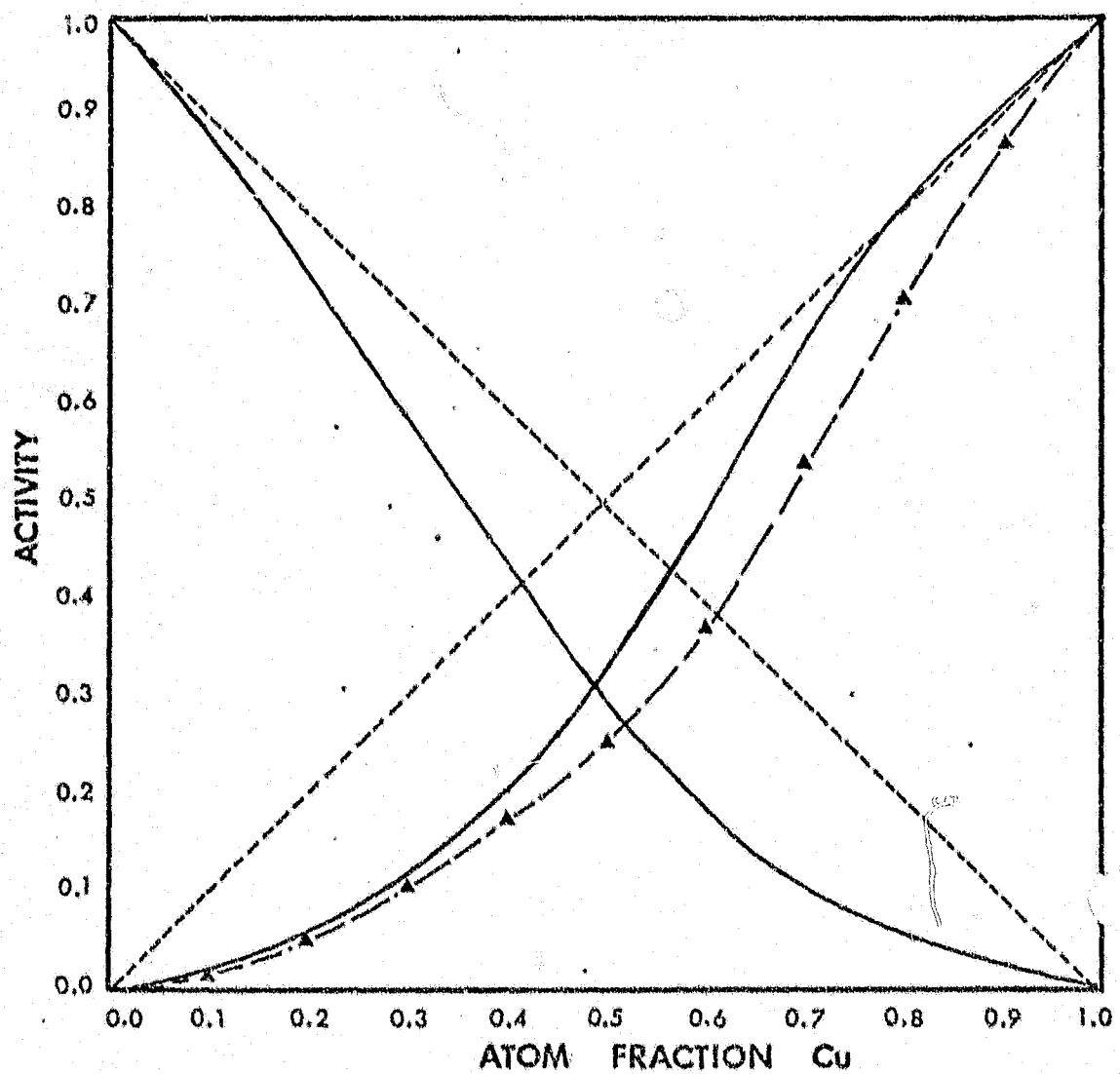


FIGURE 12 ACTIVITIES in Cu-Au LIQUID SOLUTIONS  
at 1550°K from EDWARDS and BRODSKY (34)  
▲ CALCULATED from HAGER et al (35)  
at 1573°K

and the two metals mixed to give two master alloys containing 70 and 20 mass per cent copper respectively. Each mixture was placed in a recrystallized alumina crucible in a molybdenum resistance furnace and held at  $1473^{\circ}\text{K}$  for two hours under a reducing atmosphere of deoxidized argon and hydrogen. The samples were quenched under pure argon and again turned down on a lathe. The master alloys were mixed in suitable proportions to give the other alloy compositions as required. In several runs pure copper was used.

### 3.3.3 Crucible Material

One of the greatest problems in equilibrium studies of this type is the lack of a suitable inert crucible material. The choice of refractory oxide crucibles is limited by those commercially available to either silica, alumina, magnesia or zirconia. It was decided to work at silica saturation and therefore vitreous silica crucibles were used to contain the alloy and slag. Crucible failures occurred by thermal shock and slag attack. The best crucibles were found to be thick-walled 10 ml squat crucibles (Vitreosil COO). The 10 ml crucible was contained within a 15 ml thick-walled crucible with a packing of pure precipitated silica between the two crucibles to act as a trap for slag in case of crucible failure, thereby protecting the work tube of the furnace. At  $1573^{\circ}\text{K}$  the crucibles gradually underwent a phase change from the vitreous state to a powder. At the same time the slag adhered to the crucible surface due to slag attack and thus fresh crucibles were used for each run.

### 3.4 Apparatus

This study required a system to contain slag and metal in a crucible at  $1573^{\circ}\text{K}$  for up to 40 hours under an atmosphere with a fixed oxygen potential. Facilities were required to control temperature, gas composition and to provide quenching of equilibrated samples under an inert atmosphere. The apparatus consisted of a gas train capable of delivering a controlled gas atmosphere, a reaction furnace with a quenching chamber, and accurate temperature recording and controlling equipment. These are discussed in turn.

Figure 13 is a schematic flowsheet for the apparatus whilst plates 1 and 2 are photographs of the experimental system.

#### 3.4.1 Gas Train

Three gases were used during the heating, equilibration and quenching cycle. Carbon monoxide was generated by reduction of carbon dioxide over graphite, and carbon dioxide and argon were obtained directly from cylinders. The carbon dioxide was purchased from Afrox (South Africa) and contained the following impurities.

Nitrogen	30 ppm
Oxygen	10 ppm
Water Vapour	200 ppm

Carbon dioxide from a gas cylinder was dried by passage through 98 per cent sulphuric acid and a drying column containing successive layers of calcium chloride and magnesium perchlorate (anhydrous). After drying the carbon dioxide stream was deoxidised

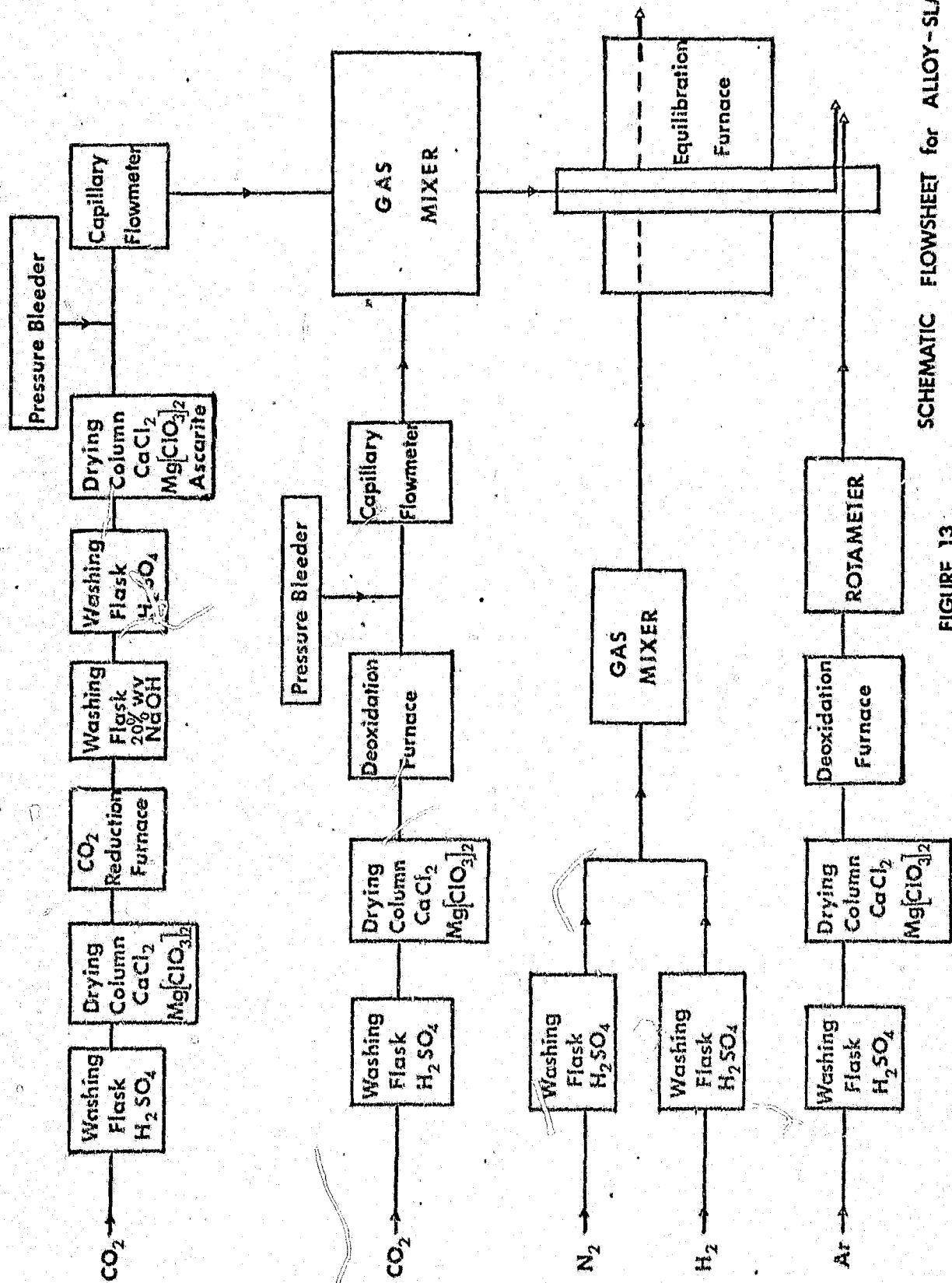
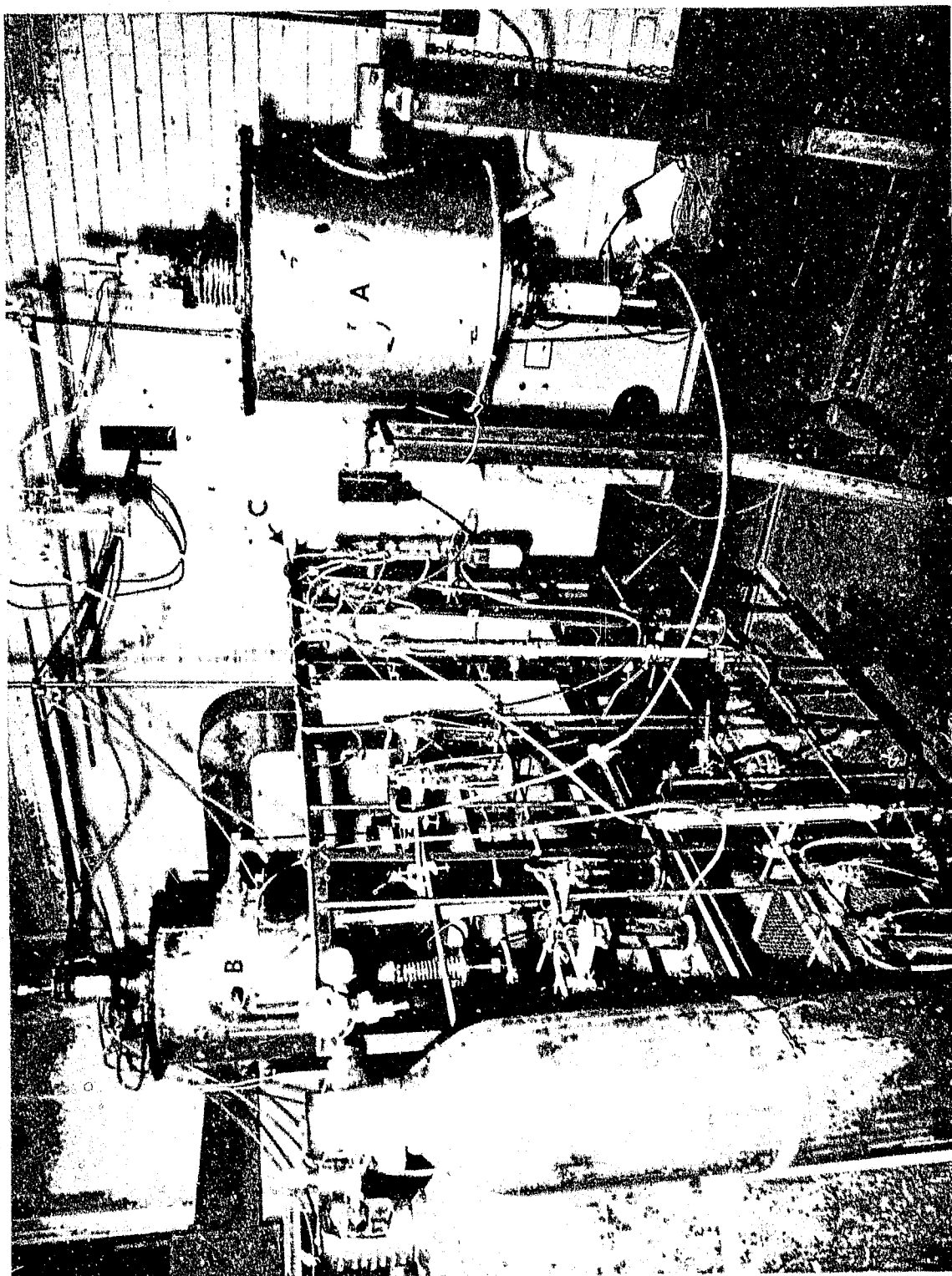


FIGURE 13  
SCHEMATIC FLOWSHEET for ALLOY-SLAG  
EQUILIBRATION SYSTEM

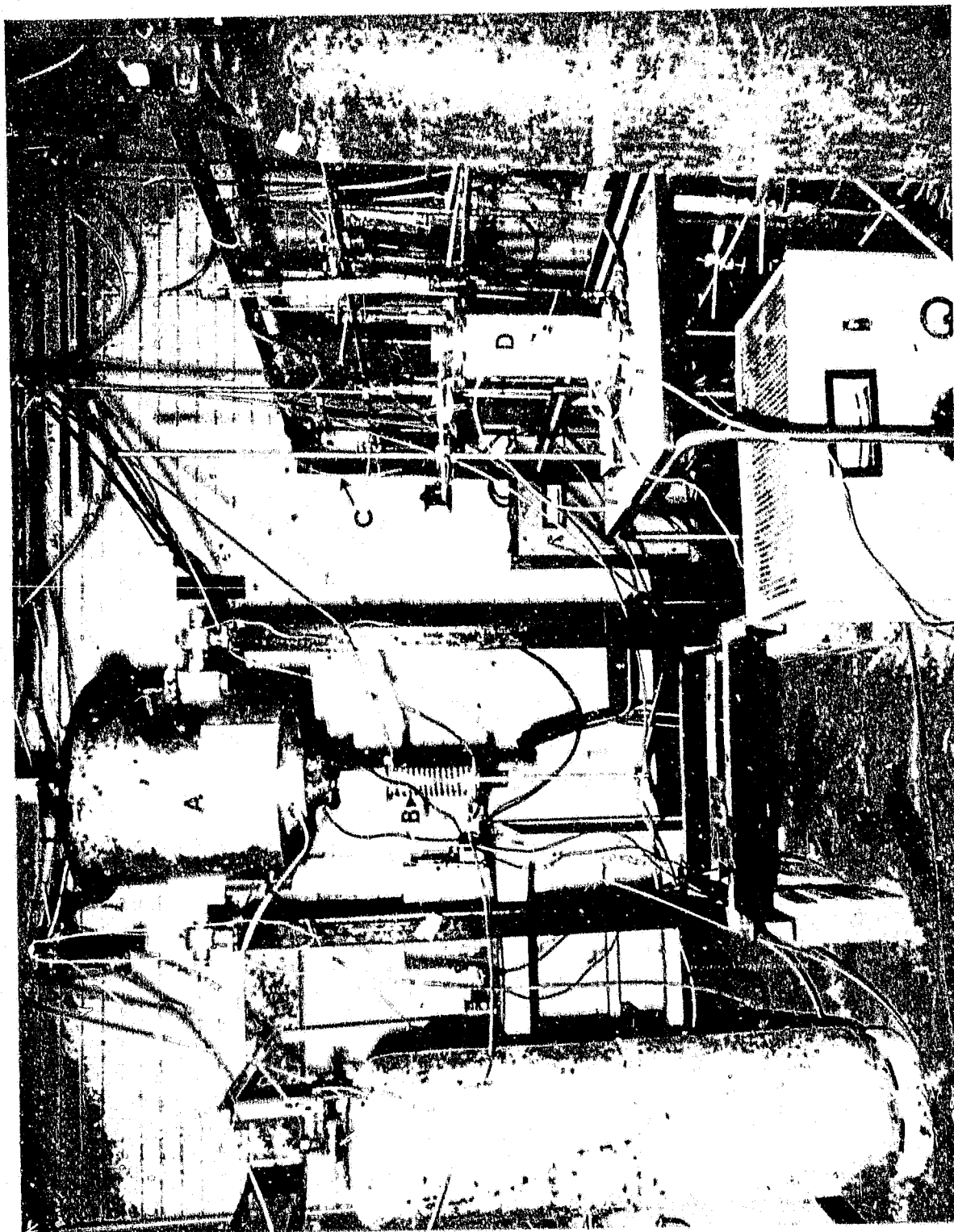


A CO<sub>2</sub> Reduction Furnace  
B Equilibration Furnace  
C Gas Train

PLATE 1.

EXPERIMENTAL SYSTEM





- |   |                       |         |
|---|-----------------------|---------|
| A | Equilibration         | Furnace |
| B | Work Tube - Quenching | Chamber |
| C | Gas Train             |         |
| D | Deoxidation           | Furnace |

PLATE 2.

EXPERIMENTAL SYSTEM



by passing it through a kanthal wound furnace containing copper turnings at a temperature of  $850^{\circ}$  K. The argon was dried and deoxidised in a similar manner.

Carbon monoxide was produced by passing carbon dioxide through a column of coarse crushed electrode graphite maintained at  $1473^{\circ}$  K in a molybdenum wound resistance furnace. The carbon monoxide generated was then passed through saturated sodium hydroxide solution to remove traces of carbon dioxide. The carbon monoxide then flowed through concentrated sulphuric acid for the removal of water vapour picked up from the NaOH solution before passing into a column containing ascarite to remove  $\text{CO}_2$  as well as calcium chloride and magnesium perchlorate to remove any remaining moisture.

The carbon dioxide and carbon monoxide gas streams each contained a gas bleeder for maintaining constant gas flow through a capillary flowmeter. The capillary flowmeters contained n-butyl phthalate as the manometric fluid and were calibrated using a soap film burette.

The carbon dioxide and carbon monoxide gas streams were intimately mixed in a gas mixer containing glass beads. The mixed gas passed to the reaction furnace where it was introduced through a 3 mm ID recrystallized alumina tube with the outlet positioned just above the crucible assembly in the furnace.

A combined flowrate of 400 cc/min of  $\text{CO}_2$  and CO was maintained through the equilibration furnace. Darken and Gurry (30) found that for a 13 mm ID tube at  $1373^{\circ}$  K a flowrate of 1.2 cm/sec was necessary to eliminate thermal diffusion of CO and  $\text{CO}_2$  and the

uncertainty in measurement of temperature was over  $1^{\circ}$  K. Thermal diffusion should be more pronounced at  $1573^{\circ}$  K and, although the experimental flowrate of 1,9 cm/sec should eliminate any thermal diffusion effects, there will be an uncertainty of over  $1^{\circ}$  K in the temperature of the hot zone. Purified argon was passed directly to the quenching chamber at a flowrate of about 1000 ml/min.

For silica-saturated iron silicate slags without any fluxing additions the  $\text{FeO-Fe}_2\text{O}_3\text{-SiO}_2$  phase diagram (31) in Figure 8 shows that as the oxygen potential is increased, the ferric ion content and hence the  $\text{Fe}^{3+}/\text{Fe}^{2+}$  ratio of the slag are increased and the silica content is generally decreased. Table 3.1 shows the variation in silica and  $\text{Fe}^{3+}$  contents and the ratio  $\text{Fe}^{3+}/\text{Fe}^{2+}$  with oxygen partial pressures from the data of Michal and Schuhmann (19).

Table 3.1 Variation of Silica,  $\text{Fe}^{3+}$  Contents and  $\text{Fe}^{3+}/\text{Fe}^{2+}$  Ratio with Partial Pressure of Oxygen

Oxygen Partial Pressure (atm)	$\text{Fe}^{3+}$ (mass %)	$\text{Fe}^{3+}/\text{Fe}^{2+}$	$\text{SiO}_2$ (mass %)
$10^{-7}$	7,9	0,164	35,0
$10^{-8}$	4,0	0,089	37,0
* $8 \times 10^{-9}$	3,3 **	0,080 **	37,9
$10^{-9}$	2,4	0,053	38,5
$10^{-10}$	1,4	0,030	39,0

\* This investigation

\*\* Run 12 deleted because of anomalous result.

The value obtained in this investigation for the  $\text{Fe}^{3+}/\text{Fe}^{2+}$  ratio in silica-saturated slag containing no flux additions was 0.090. This compares with the expected value of  $\text{Fe}^{3+}/\text{Fe}^{2+} = 0.0811$  at an oxygen partial pressure of  $8 \times 10^{-19}$  atm (19). The result indicates that accurate atmosphere control was maintained throughout the experiments.

#### 3.4.2 Furnace Assembly

A molybdenum resistance furnace with a constant temperature zone of approximately 50 mm was used as the equilibration furnace. A scale diagram of the furnace assembly is shown in Figure 14. 1 mm gauge molybdenum wire was wound on a porous alumina tube at a spacing which could give a maximum operating temperature of  $1773^\circ \text{K}$ . The element was held in place by alumina cement and alumina bubble served as an insulating medium between the element and an outer porous alumina tube. Refractory brick was used as packing between this tube and the furnace shell. The furnace was sealed at top and bottom against the work tube and a mixture of four parts of nitrogen to one part of hydrogen was introduced through the furnace shell to prevent oxidation of the molybdenum wire at temperature.

The constant heat zone was maintained at  $1573^\circ \pm 2.5^\circ \text{K}$  over a height of 45 mm within the work tube. The overall temperature drift was reduced to  $\pm 2^\circ \text{K}$  using a Eurotherm thyristor controller.

A molybdenum furnace was used because it was the only type available at the time. There is the risk that reducing gas from the furnace casing can diffuse through the work tube and upset the controlled value of oxygen partial pressure. However, the results

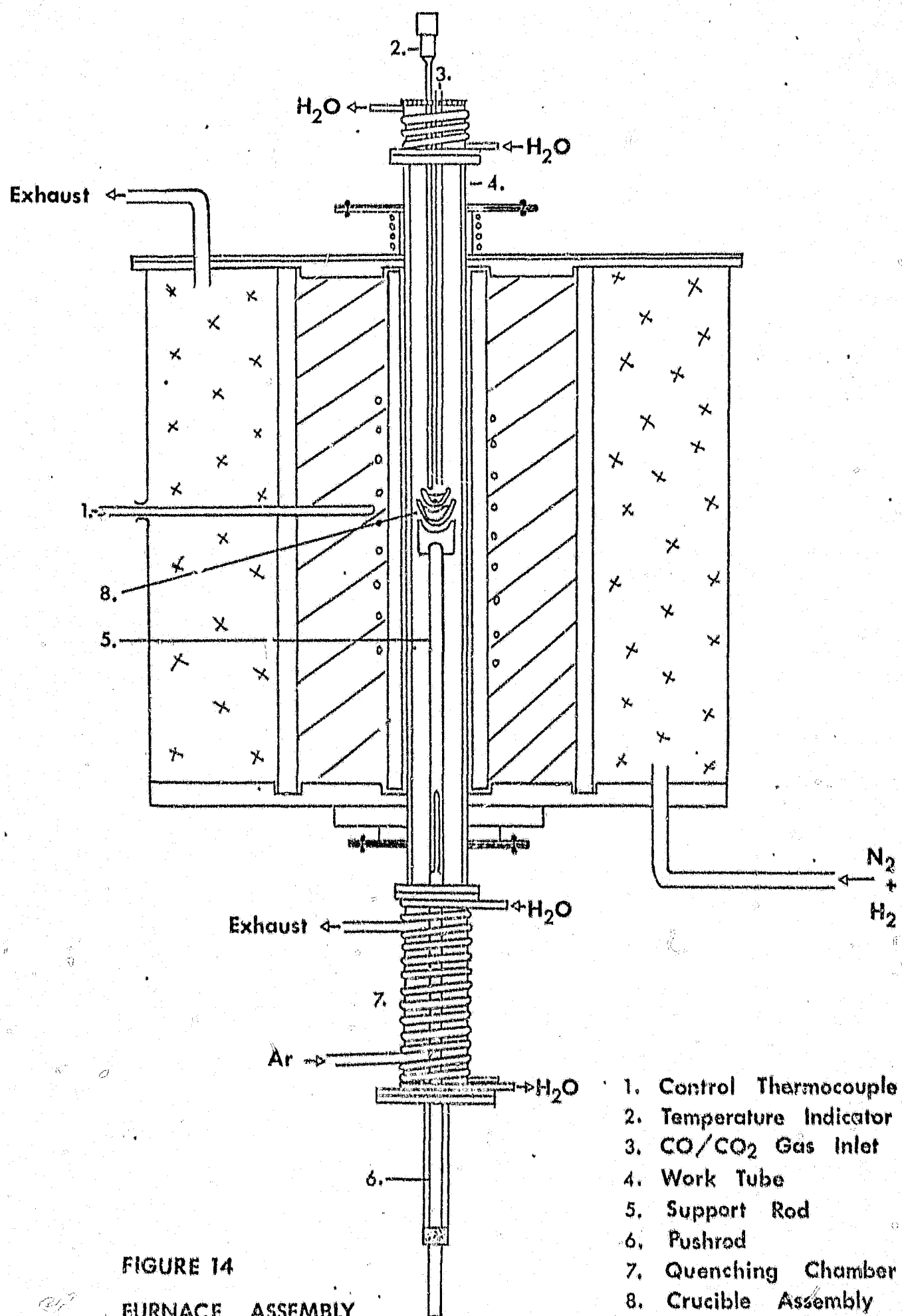
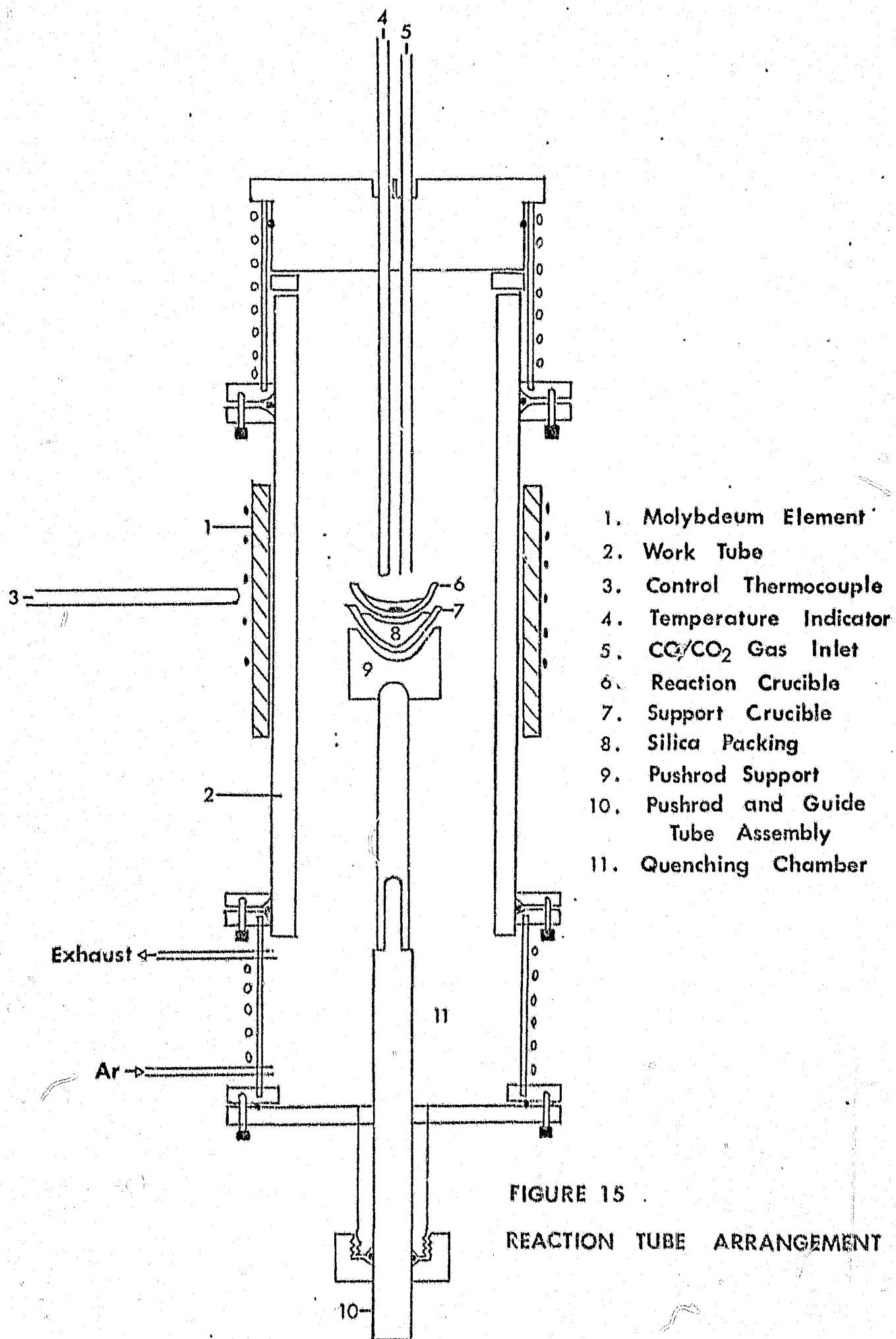


FIGURE 14  
 FURNACE ASSEMBLY

for flux-free slags are consistent with results of previous investigators. Therefore it is concluded that diffusion of reducing gas into the work tube did not occur.

The work tube arrangement is shown in more detail in Figure 15 and consisted of a recrystallized pythagoras tube sealed at both ends with water cooled jackets. The work tube was 1000 mm in length with OD 60 mm and ID 50 mm. The tube was kept in position in the furnace using a mixture of asbestos string and Volar industrial lubricant compacted between the tube and the top and bottom furnace flanges. The sheath at the top of the work tube was sealed at the flange by rubber O-rings. The gas inlet and thermocouple sheath were set into a removable brass block at the top of the sheath using silicone rubber. The lower jacket was sealed to the work tube in a similar fashion to that of the upper jacket and opened out into a quenching chamber which incorporated an argon inlet and exhaust for the CO/CO<sub>2</sub> gas mixture. The silica crucible assembly rested on top of a base of alumina cement supported by a recrystallized alumina rod. The arrangement is shown in Figure 16 and Plate 3. Only one reaction crucible could be used during each run because of the diameter of the work tube.

The crucible assembly was supported within the hot zone by a recrystallized alumina tube (5 mm ID) which slotted onto a stainless steel pushrod (10 mm OD). The pushrod passed downward through the quenching chamber into a brass guide tube which was screwed to the base of the quenching chamber against an O-ring to form a gas tight seal. A threaded screw seal held the pushrod in position within the furnace and when this seal was unscrewed slightly it was possible to smoothly raise or lower the crucible assembly by hand.



1. Temperature Indicator
2. CO/CO<sub>2</sub> Gas Inlet
3. Reaction Crucible  
Vitrosil COO
4. Support Crucible
5. Silica Packing
6. Iron Silicate Slag
7. Cu - Au Alloy
8. Work Tube
9. Support Rod
10. Cast Alumina  
Support

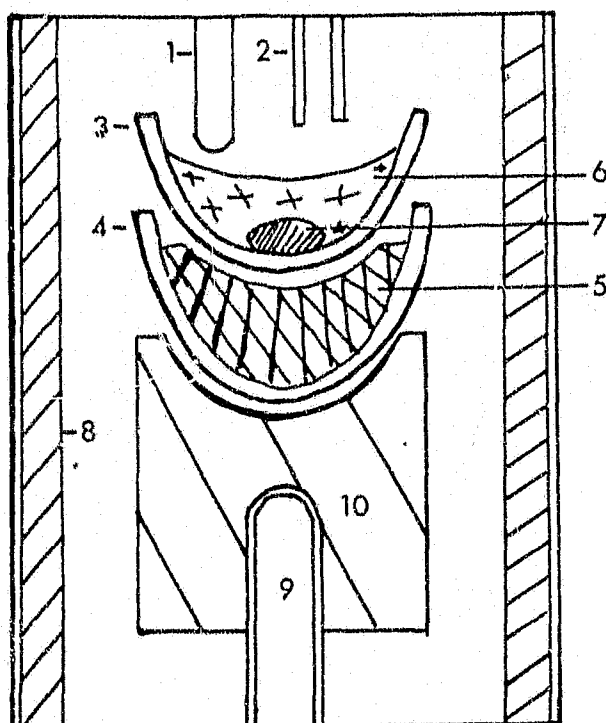


FIGURE 16.

## CRUCIBLE ARRANGEMENT

- A Charge
- B Reaction Crucible
- C Support Crucible
- D Alumina Support

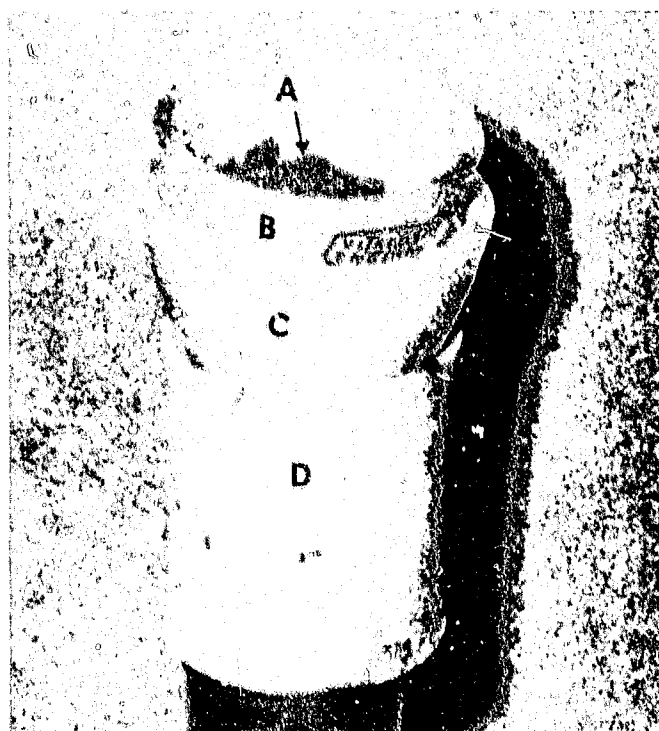


PLATE 3.

## CRUCIBLE ASSEMBLY



The temperature in the furnace was measured using a Pt/Pt-13% Rh thermocouple positioned 10 mm above the slag surface in the crucible. The e.m.f. output, relative to an ice-water mixture, was displayed on a Hewlett-Packard digital multimeter. A Hitachi flat bed recorder was used to record temperature drift and was adjusted to 1mV full scale using an electronic "back-off" unit. A schematic diagram of the circuit is shown in Figure 17.

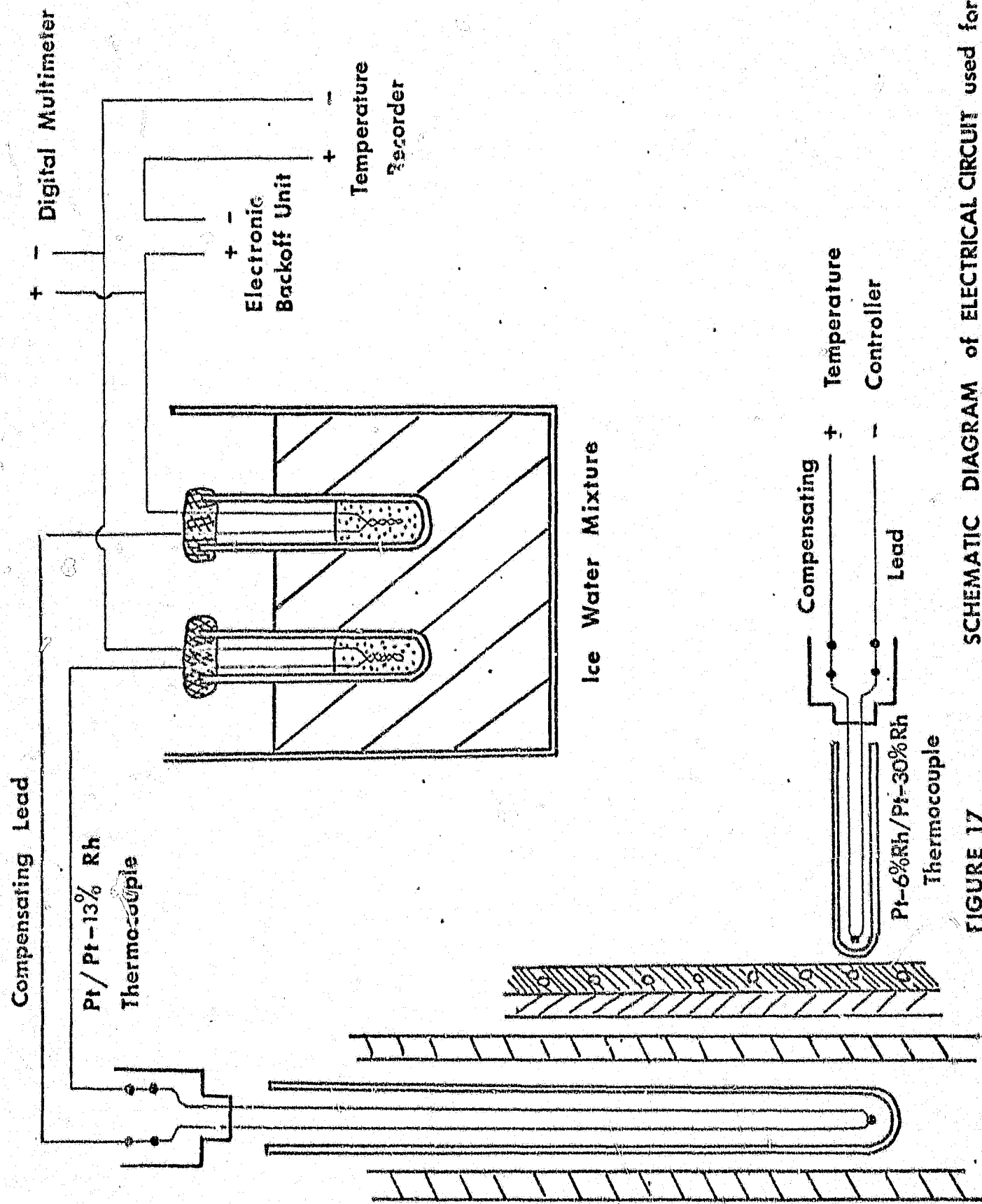
The temperature was controlled by a 1% Rh/Pt-30% Rh thermocouple positioned 3 mm from the molybdenum resistance element connected to a 25 amp maximum capacity Eurotherm three term thyristor controller.

Both thermocouples were checked against standard thermocouples calibrated at the melting points of copper and nickel.

### 3.5 Procedure

A standard charge of 2 g of alloy and 5 g of slag was weighed out for each experiment. For experiments involving additions of magnesia, alumina or lime the required amounts of either  $MgO$ ,  $Al_2O_3$  or  $CaO$  were weighed out and mixed with the slag. The crucible arrangement was then placed on top of the guide tube which was positioned and sealed to the base of the quenching chamber. The furnace tube was flushed for 20 minutes before the crucible assembly was raised 20 cm and sealed around the stainless steel pushrod by tightening the threaded screw. The furnace tube was flushed for a further 10 minutes and then the crucible assembly was raised in





SCHEMATIC DIAGRAM of ELECTRICAL CIRCUIT used for  
ALLOY-SLAG EQUILIBRATIONS

FIGURE 17

stages of 10 cm over five minute intervals until it was in position. Once the crucible assembly was in position the CO/CO<sub>2</sub> gas mixture was switched from bypass into the furnace and the flushing gas was turned off. The hot zone reattained temperature after approximately 15 minutes and the sample was maintained at temperature for a period of 25 hours. Any final adjustment to the CO/CO<sub>2</sub> ratio was made by varying the pressure head in the bleeders. Temperature and flowrates normally remained steady throughout the experiment.

At the end of the equilibration period argon was flushed into the quenching chamber, the CO/CO<sub>2</sub> gas mixture turned to bypass, and the crucible assembly quickly lowered into the chamber. The sample was allowed to cool within the chamber for 15 minutes before removal from the furnace.

### 3.6 Analytical Techniques

This section discusses preparation and analysis of alloy and slag samples. Care was taken to obtain representative samples. The alloy was analysed for copper, gold and iron whilst the slag was analysed for copper, gold, total iron, ferrous ion (II), silica, magnesia, alumina and lime where applicable.

#### 3.6.1 Preparation of Samples for Analysis

After the sample was removed from the quenching chamber, the slag and alloy phases were separated and cleaned for analysis. The crucible wall above the slag line was easily broken away and

the remaining sample broken into small particles thus releasing the alloy phase. Slag adhering to the alloy phase would cause high iron values and thus the beads were cleaned using an electrically driven stiff wire wheel. The beads were then carefully turned down using a Bridgeport milling machine.

Grinding on an electric grinding wheel proved the most effective method for removing the crucible wall from the slag. Clean separation was achieved because of the noticeable difference in texture between the two phases and any contamination of the slag with crucible material was avoided. Any fine alloy particles adhering to the slag were also removed by grinding. The slag particles were then ground in a Siebtechnik mill.

Analyses were carried out by the Analytical Division of The National Institute for Metallurgy, Johannesburg.

### 3.6.2 Analysis of Alloy

Copper (36) was determined by the short iodine procedure and interference from iron was prevented by complexation with ammonium bifluoride. 0,5 g of alloy was dissolved in a mixture of nitric and sulphuric acids, boiled to remove oxides of nitrogen and fumed. The solution was neutralised in ammonium hydroxide and reacidified using acetic acid. Potassium iodide was added and the solution titrated with standard sodium thiosulphate solution.

Gold (37) was finally removed by normal fire assay. Base metals were first removed by scorification. Between 1 to 5 g of alloy was wrapped in assay Pb foil and placed in a scorifying dish. The sample

was finally analysed as a standard gold sample.

Iron (38) was determined by atomic absorption spectroscopy. 1 g of alloy was dissolved in an  $\text{HCl}/\text{HNO}_3/\text{H}_2\text{O}$  mixture and diluted to standard volume using potassium nitrate.

### 3.6.3 Analysis of Slag

For analysis of iron (FeII), (39) the sample was dissolved in a  $\text{HF}/\text{H}_2\text{SO}_4$  mixture in the presence of excess sodium metavanadate. The hydrofluoric acid was then complexed with boric acid and the unreacted vanadium  $\text{V}$  titrated with standard ferrous ammonium sulphate solution using sodium diphenylamine sulphonate as the redox indicator.

After dissolution of the slag, gold was separated and concentrated by liquid-liquid extraction and determined directly by atomic absorption spectroscopy. From the organic phase 5 g of sample was digested in aqua regia. The solids were taken up in  $\text{HCl}$  and diluted to volume. A suitable aliquot was extracted into 5 ml of Aliquot 335-DISK solution. If the gold was sufficiently high it was determined directly in the aqueous phase by atomic absorption spectroscopy as described below for copper.

For analysis of copper 0.5 g of sample was heated with  $\text{HF}/\text{HClO}_4$  mixture. The residue was treated with fresh aqua regia if gold was also to be determined. One ml of  $\text{HCl}$  was added and the solution diluted to standard volume. Copper was determined directly from the clear solution by atomic absorption spectroscopy.

Total iron, silica,  $\text{MgO}$ ,  $\text{Al}_2\text{O}_3$  and  $\text{CaO}$  (40, 41) were determined by X-Ray fluorescence spectrometry. 1 g of the slag sample was fused with lithium tetraborate/LiF/sodium tetraborate flux in a platinum crucible and the mass dilution ratio determined. The flux was cast into a glass disc and the intensity of each element determined by X.R.F. Single element standards in the same flux were used and corrections for inter-element effects in the sample were made using pre-determined influence factors.

#### 4. RESULTS

In this section the experimental results are tabulated as the mass per cent of copper, gold and iron in the alloy and the slag composition as the mass per cent of the respective oxide components. The time required to establish equilibrium is given.

##### 4.1 Equilibration Time

The period required to establish equilibrium was determined by contacting 2 g of copper-gold alloy containing 70,9 mass per cent copper with 5 g of fayalite slag. The samples were held at 1573° K under an oxygen partial pressure of  $8 \times 10^{-9}$  atm. The results are shown in Figure 18 and Table 4.1 and indicate that equilibrium was achieved within about 20 hours. In all subsequent runs the samples were held at temperature for 25 hours to ensure that equilibrium was attained.

Table 4.1

Copper Content of Slag for Different  
Contacting Times

Temperature 1573° K

Oxygen partial pressure  $8 \times 10^{-9}$  atm

Alloy copper content 70,94 mass per cent

Run No.	Time (hours)	Copper in Slag (mass per cent)
2	5	1,3
3	10	1,9
5	20	2,0
7	25	2,1
42	40	2,12

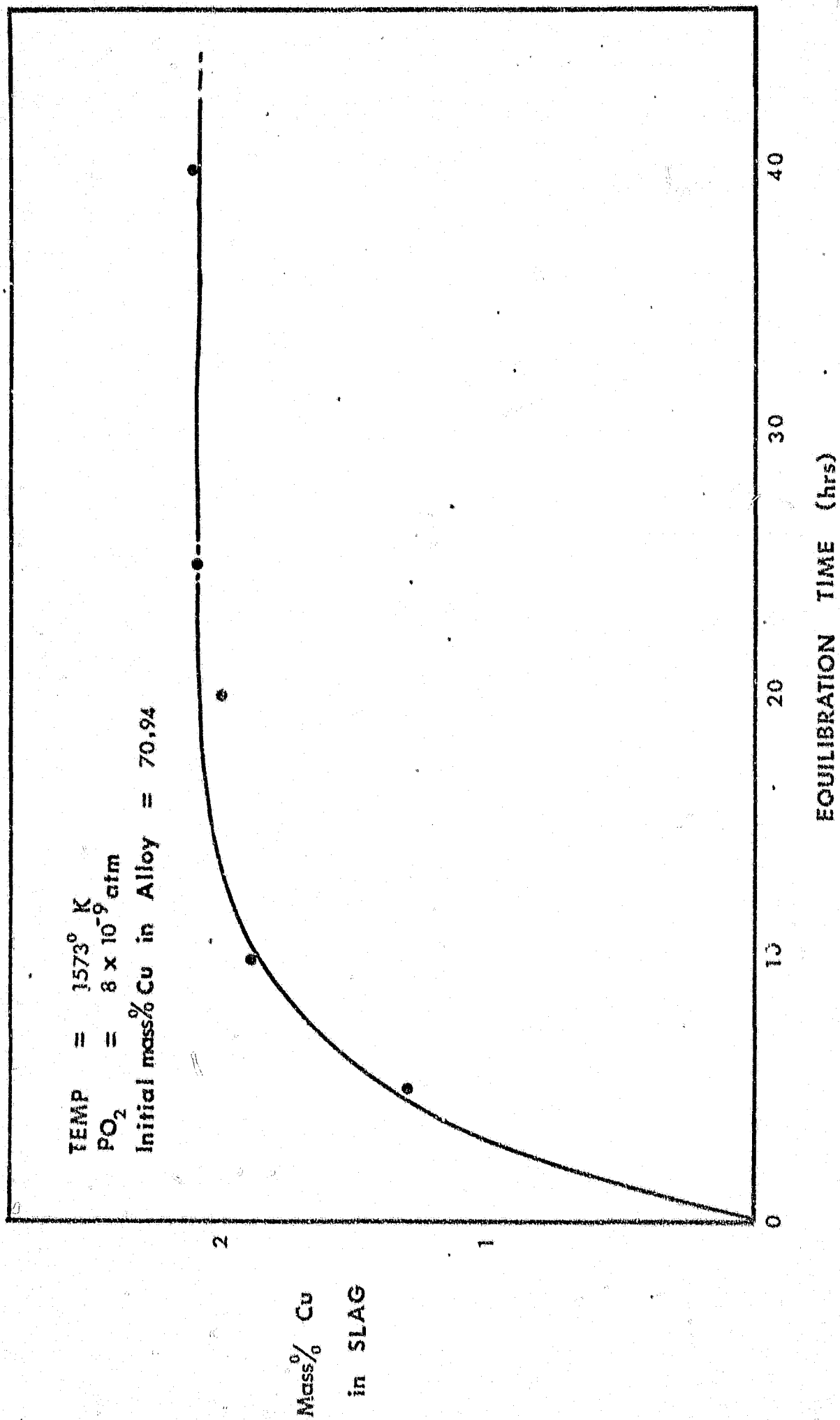


FIGURE 18  
 COPPER DISSOLVED in SILICA-SATURATED SLAG  
 as a FUNCTION of CONTACTING TIME



#### 4.2 Copper Solubility in Iron Silicate Slag

The analyses of the slag and the alloy for experiments without fluxing additions are tabulated in Table 4.2. The alloy was analysed for copper, gold and iron and the analysis smoothed to 100 mass per cent. The slag was analysed for copper, gold, total iron, ferrous iron and silica. The analytical data for the slag have been expressed as unsmoothed mass percentages of the oxides  $\text{Cu}_2\text{O}$ ,  $\text{FeO}$ ,  $\text{Fe}_2\text{O}_3$  and  $\text{SiO}_2$ . (Smoothing was not necessary at this stage as this would be effectively accomplished when calculating mole fractions). Total iron and ferrous iron could only be analysed to within  $\pm 5\%$  of the amount present. All other analyses are accurate to  $\pm 2\%$  of the amount present. The analyses of the alloy had a combined error (Cu, Au, Fe) of  $\pm 2\%$ .

In all experiments the gold content of the slag was less than 0.01 mass per cent. The solubility of gold in fayalite slag at  $1573^\circ \text{K}$  is very small (0.008 mass per cent). (18) No correlation between gold and copper contents was observed (Figure 19) which suggested that very little, if any, copper was present in the slag as entrained alloy.

As the copper content of the alloy was varied from 19.7 to 99.9 mass per cent the copper oxide content varied from 0.56 to 2.71 mass per cent. The  $\text{Fe}_2\text{O}_3$  and  $\text{SiO}_2$  contents remained relatively constant apart from one anomaly in Run 12.



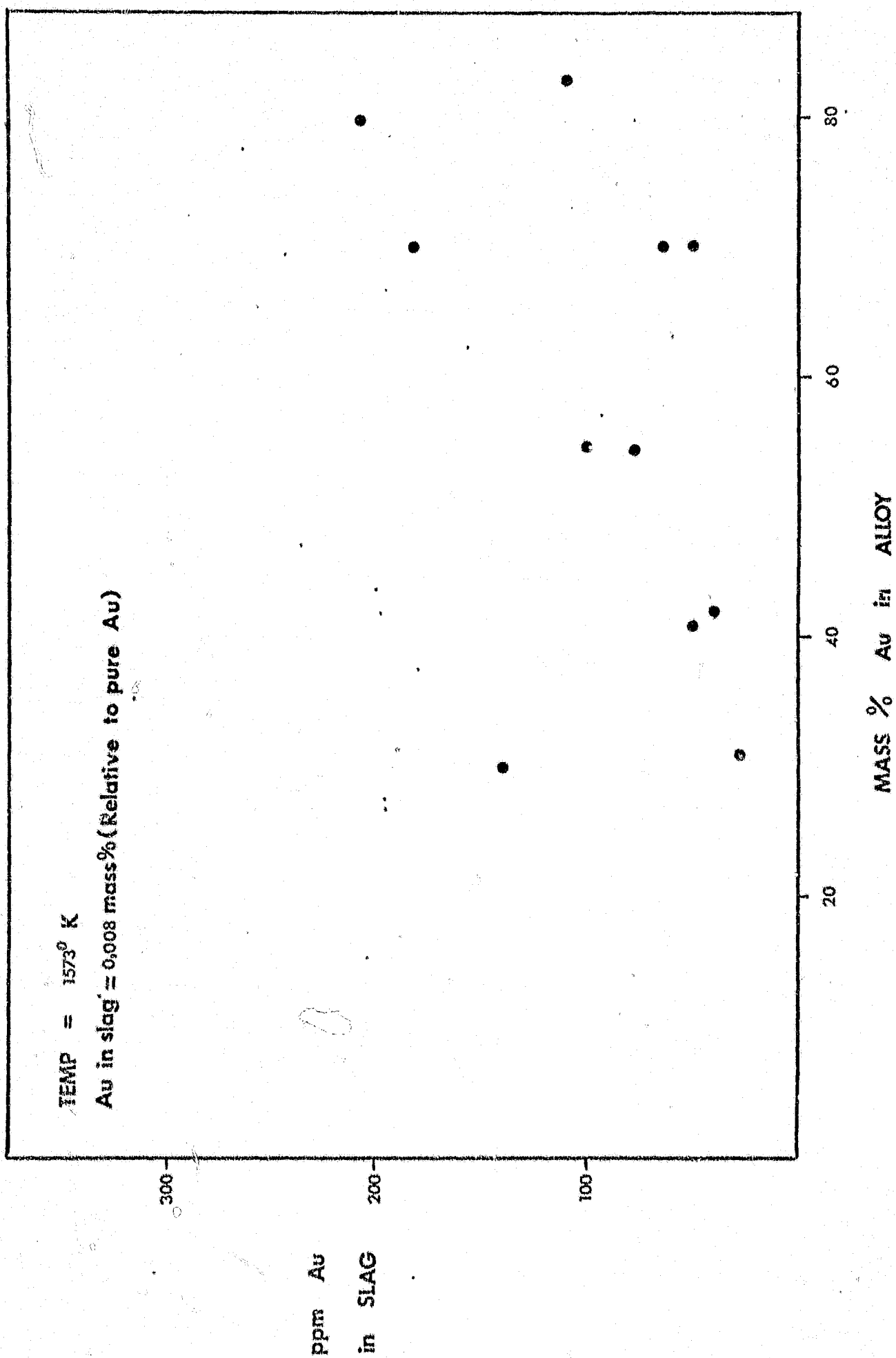


FIGURE 10 GOLD CONTENT OF SLAG for DIFFERENT RUNS

#### 4.3 Copper Solubility in Iron Silicate Slag With Fluxing Additions

The analyses of the slag and alloy for slags containing fluxing additions are tabulated in Table 4.2. For all fluxing additions the alloy was analysed for copper, gold and iron and the analysis smoothed to 100 mass per cent. The slag phase was analysed for copper, gold, total iron, ferrous iron, silica, and magnesia, alumina and lime where appropriate. The analytical data have been expressed as mass percentages of the respective oxides.

Addition of 4,0 mass per cent magnesia was observed to increase the silica content to 39,3 mass per cent, and decrease the total iron oxide content to 52,3 mass per cent compared to values of 37,9 and 58,2 mass per cent respectively for the runs without fluxing additions. As the copper content of the alloy varied from 19,98 to 99,97 mass per cent the copper oxide content of the slag varied from 0,51 to 2,50 mass per cent.

For the addition of 8,0 mass per cent alumina the copper oxide content varied from 0,54 to 2,13 mass per cent whilst the copper content of the alloy varied from 18,0 to 58,0 mass per cent. The average silica and total iron contents were 43,3 and 47,4 mass per cent respectively. Two experiments at 4,3 mass per cent alumina were also carried out at copper contents in alloy of 55,7 and 68,6 per cent.

For lime additions three series of experiments were completed. The lime contents of the slag were fixed at 4,3 , 7,5 and 10,5 mass per cent  $\text{CaO}$ . Over this range the silica content was observed to vary from 41,0 to 44,0 and to 45,4 mass per cent while the total iron varied from 51,5 to 45,6 and 41,6 mass per cent respectively.

With increasing lime additions, the copper content of the alloy for each series varied from 18,8 to 69,5 from 18,5 to 66,8 and from 18,6 to 65,9 mass per cent as the copper oxide contents varied from 0,47 to 2,13 from 0,35 to 1,85 and from 0,32 to 1,58 mass per cent respectively..

TABLE 4.2 PRESENTATION OF RAW DATA FOR ALLOY AND SLAG COMPOSITION

Run No.	Alloy Composition (mass per cent)						Slag Composition (mass per cent)							
	Cu	Au	Fe	Smoothering Factor	Cu	Cu <sub>2</sub> O	Au	FeO	Fe <sub>2</sub> O <sub>3</sub>	Fe <sup>3+</sup> /Fe <sup>2+</sup>	SiO <sub>2</sub>	MgO	Al <sub>2</sub> O <sub>3</sub>	CaO
12	19,68	79,82	0,50	1,001	0,50	0,56	0,01	51,33	8,34	0,146	37,7			
44	29,91	69,96	0,10	1,003	0,87	0,98	0,01	53,52	5,49	0,092	38,64			
10	42,55	57,35	0,10	1,327	1,50	1,69	0,01	54,68	4,58	0,075	36,9			
55	53,73	46,17	0,10	0,9967	1,72	1,94	0,01	51,72	5,36	0,093	38,86			
7	68,73	31,17	0,10	1,017	2,10	2,36	0,01	53,84	4,25	0,071	36,1			
53	99,90	-	0,10	0,9988	2,41	2,71	0,01	51,97	3,95	0,069	39,35			

MAGNESIA ADDITIONS

13	18,98	80,87	0,15	1,0276	0,45	0,51	0,01	47,99	4,79	0,090	39,40	3,99		
14	31,52	68,40	0,08	1,0088	0,89	1,00	0,01	47,34	5,72	0,109	40,10	3,97		
15	45,31	54,64	0,05	1,0175	1,22	1,37	0,01	48,12	4,29	0,080	40,40	3,86		
16	57,49	41,67	0,04	1,0094	1,81	2,04	0,01	48,31	3,22	0,060	40,00	3,61		
17	69,87	30,10	0,03	1,0033	2,22	2,50	0,01	48,37	4,50	0,084	39,70	3,35		
56	99,97	-	0,03	0,9980	2,20	2,48	0,01	47,28	4,07	0,076	36,18	3,37		

TABLE 4.2 cont.

## PRESENTATION OF RAW DATA FOR ALLOY AND SLAG COMPOSITION

Alloy Composition (mass per cent)					Slag Composition (mass per cent)									
Run No.	Cu	Au	Fe	Smoothing Factor	Cu	Cu <sub>2</sub> O	Au	FeO	Fe <sub>2</sub> O <sub>3</sub>	Fe <sup>3+</sup> /Fe <sup>2+</sup>	SiO <sub>2</sub>	MgO	Al <sub>2</sub> O <sub>3</sub>	CaO
ALUMINA ADDITIONS														
19	55,73	44,23	0,04	0,9994	1,77	1,99	0,01	49,27	4,72	0,086	41,25		4,10	
18	68,55	31,42	0,03	0,9963	2,14	2,41	0,01	49,27	4,58	0,084	40,09		4,55	
24	17,97	81,93	0,10	1,0070	0,476	0,54	0,01	44,51	3,43	0,069	42,64		8,37	
25	31,11	68,82	0,07	0,9837	0,815	0,92	0,01	44,32	3,79	0,077	43,26		8,11	
26	42,50	57,45	0,06	1,0026	1,31	1,47	0,01	43,74	3,57	0,074	43,50		8,48	
57	53,72	46,16	0,12	0,9969	1,70	1,91	0,01	42,58	3,29	0,069	43,57		7,08	
28	57,72	41,98	0,05	0,9575	1,845	2,08	0,01	43,87	4,00	0,082	43,60		8,32	
LIME ADDITIONS														
38	18,80	81,07	0,13	1,0053	0,42	0,47	0,01	47,34	5,12	0,097	42,51		4,41	
36	31,47	68,45	0,08	1,0138	0,87	0,98	0,01	48,63	3,26	0,060	42,12		4,51	
37	40,82	59,13	0,05	1,0045	1,30	1,46	0,01	48,24	2,63	0,049	38,79		4,33	
34	52,63	47,30	0,07	0,9937	1,62	1,82	0,01	47,41	4,02	0,076	39,74		4,19	
33	69,42	30,44	0,04	1,0069	1,89	2,13	0,01	47,60	3,17	0,060	41,94		4,46	

PRESENTATION OF RAW DATA FOR ALLOY AND SLAG COMPOSITION

TABLE 4.2 cont.

Alloy Composition (mass per cent)										Slag Composition (mass per cent)				
Run No.	Cu	Au	Fe	Smoothering Factor	Cu	Cu <sub>2</sub> O	Au	FeO	Fe <sub>2</sub> O <sub>3</sub>	Fe <sup>3+</sup> /Fe <sup>2+</sup>	SiO <sub>2</sub>	MgO	Al <sub>2</sub> O <sub>3</sub>	CaO
LIME ADDITIONS														
50	18,53	81,35	0,12	1,0092	0,31	0,35	<0,01	41,43	4,99	0,108	45,19			7,91
49	30,44	69,49	0,07	1,0087	0,73	0,82	<0,01	41,94	4,72	0,101	44,36			7,65
52	40,40	59,54	0,06	0,9951	1,08	1,22	<0,01	41,81	3,07	0,066	43,76			7,63
51	54,76	45,17	0,07	1,0007	1,43	1,61	<0,01	42,84	1,87	0,039	44,45			7,69
45	66,79	33,15	0,06	0,9986	1,64	1,85	<0,01	42,84	2,33	0,049	42,01			7,49
41	18,62	81,25	0,13	1,0043	0,28	0,32	<0,01	39,11	3,86	0,089	46,51			10,64
40	31,42	68,47	0,11	1,0121	0,67	0,75	<0,01	38,60	3,03	0,071	42,78			10,05
32	43,32	56,61	0,07	1,0087	0,99	1,11	<0,01	37,95	3,30	0,078	45,88			10,59
39	56,03	43,89	0,08	1,0048	1,33	1,50	<0,01	38,21	2,90	0,068	46,55			10,79
30	65,90	34,06	0,04	0,9954	1,40	1,58	<0,01	38,85	1,93	0,045	45,23			10,56

## 5. SOLUBILITY OF COPPER IN SILICA-SATURATED IRON SILICATE SLAGS

### 5.1 No Fluxing Additions

The solubility of copper in the silica-saturated slag without fluxing additions is shown in Figure 20 as mass per cent copper in the slag versus mass per cent copper in the alloy. The copper solubility in the slag increases with increasing copper content of the alloy to a maximum of 2.4 mass per cent copper when the slag is equilibrated with pure copper. Values from this investigation have been compared with those of Ruddle et al (8) and Toguri and Santander (17) in Figure 20.

The experimental point of Ruddle et al for pure copper at silica-saturation appears to be a little high and is possibly a result of entrainment of copper in the slag. The results of Toguri and Santander are also higher at high copper contents in the alloy and this may be due to either entrapment of the alloy in the slag (unlikely) (21) or to the slightly higher oxygen partial pressure. The values at copper contents of the alloy up to 50 mass per cent are lower and this may be due to the effect of about 6 mass per cent alumina in the slag. However, the general agreement between this investigation and previous studies is very good and indicates that the experimental system operated correctly.

Molybdenum wound furnaces with reducing gas surrounding the elements were used for this study. There is the possibility that





this gas may diffuse through the work tube and hence alter the partial pressure of oxygen in the vicinity of the reaction crucible. However, because of the satisfactory agreement between this and previous studies this does not appear to have occurred in this case.

#### 5.1.1 Solubility of Copper as $\text{CuO}_{0.5}$

The solubility data were analysed using a thermodynamic approach that involves the calculation of the activity of copper oxide in the slag as  $\text{CuO}_{0.5}$ .

Although the oxidation state of copper cannot be determined by analytical methods there is indirect evidence to support the view that dissolved copper exists in the molten state predominantly as the cuprous species rather than the cupric species. It has been assumed that the copper dissolved in the slag exists solely as the cuprous species.

Slags are ionic solutions (46, 47) and copper oxide may exist in slag as  $\text{Cu}^+$  or  $\text{Cu}_2^{++}$  ions or as a more complex ion involving other slag components (18). Lumsden (47) has suggested that the properties of simple iron silicate slags can be more conveniently described using a composition based on the neutral oxides  $\text{FeO}$ ,  $\text{FeO}_{1.5}$  and  $\text{SiO}_2$ . The species  $\text{FeO}_{1.5}$  is introduced because the ferric species in the slag is the mononuclear ion  $\text{Fe}^{3+}$ .

Using a similar concept to introduce the species  $\text{CuO}_{0.5}$  the two possible mechanisms for copper dissolution in slag are given

by the equations



$$\text{where } a_{\text{Cu}_2\text{O}} = K_1 a_{\text{CuPO}_2}^2 \quad 5.3$$

$$\text{and } a_{\text{CuO}_{0.5}} = K_2 a_{\text{CuPO}_2} \quad 5.4$$

Altman and Kellogg (18) provided firm evidence for the existence of the species  $\text{CuO}_{0.5}$  by plotting the activity coefficients of  $\text{Cu}_2\text{O}$  and  $\text{CuO}_{0.5}$  versus the mole fractions of  $\text{Cu}_2\text{O}$  and  $\text{CuO}_{0.5}$ . (Figure 21). It is evident from the figure that the species  $\text{CuO}_{0.5}$  exhibits a mild positive deviation from ideal behaviour and that  $\gamma_{\text{CuO}_{0.5}}$  approaches a constant value as  $N_{\text{CuO}_{0.5}}$  approaches zero. Both these observations are consistent with the species  $\text{CuO}_{0.5}$  obeying Henry's law at low concentrations of  $\text{CuO}_{0.5}$  in the slag. In contrast the  $\text{Cu}_2\text{O}$  species exhibits a strong negative deviation from ideal behaviour and  $\gamma_{\text{Cu}_2\text{O}}$  tends to zero as  $N_{\text{Cu}_2\text{O}}$  approaches zero. This implies that the species  $\text{Cu}_2\text{O}$  does not obey Henry's law. The negative deviation might occur because of the presence of copper complexes in the slag but there is no evidence for the existence of such complexes (21).

Earlier work by Toguri and Santander (17) also provides evidence for the existence of the species  $\text{CuO}_{0.5}$ . Temkin's model for the behaviour of ionic slag species was used to show that

$$(\text{mass \% Cu in slag}) \propto \sqrt{K_1} a_{\text{CuPO}_2} \quad 5.5$$

$$\begin{aligned} \text{where } a_{\text{Cu}_2\text{O}} &\propto (\text{mass \% Cu in slag})^2 \quad 5.6 \\ &= N_{\text{Cu}^+}^2 N_{\text{O}^{2-}} \gamma_{\text{Cu}_2\text{O}} \end{aligned}$$

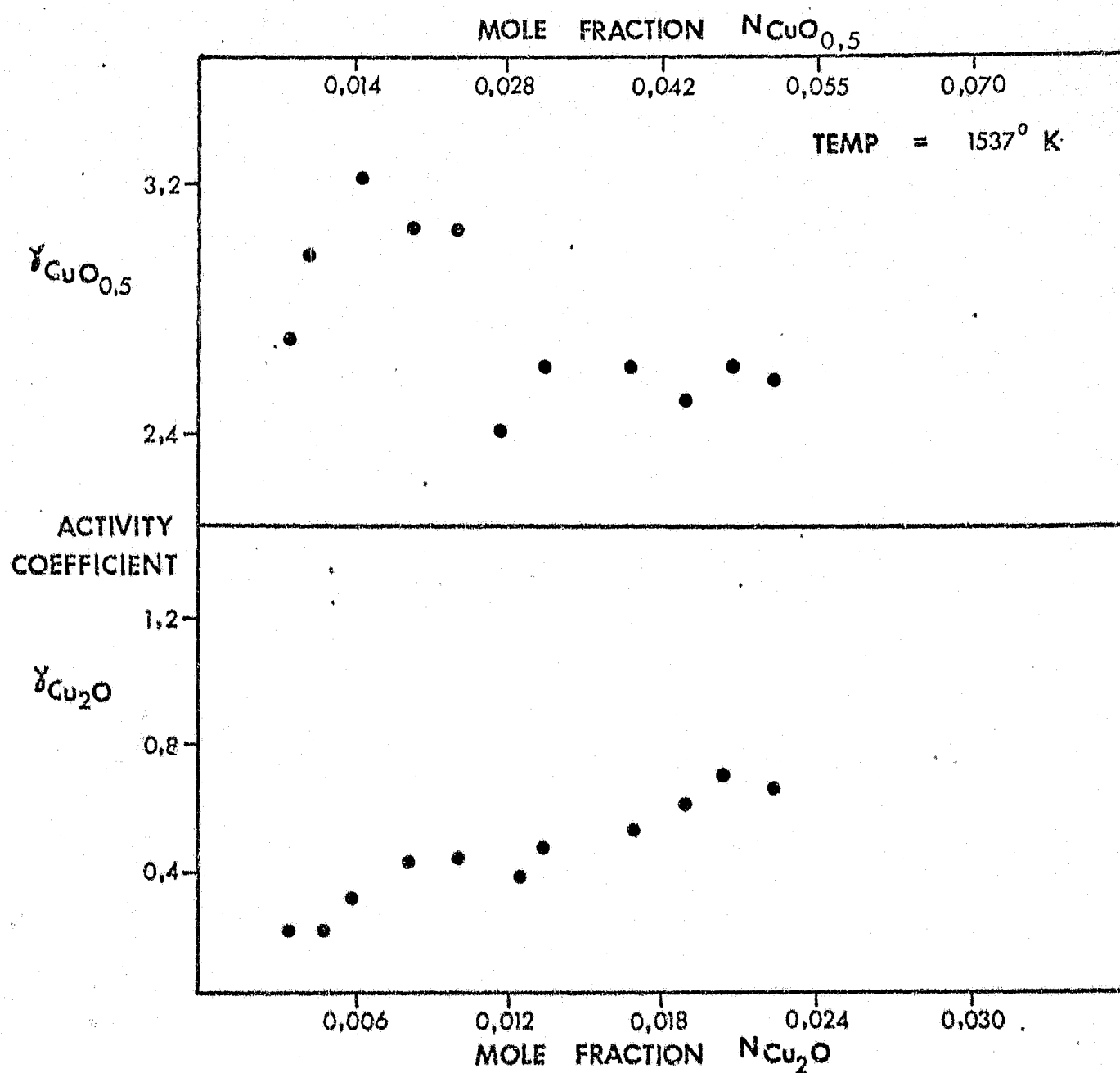


FIGURE 21

ACTIVITY COEFFICIENTS of  $\text{Cu}_2\text{O}$  and  $\text{CuO}_{0.5}$  VERSUS  
MOLE FRACTIONS of  $\text{Cu}_2\text{O}$  and  $\text{CuO}_{0.5}$

Pure liquid  $\text{CuO}_{0,5}$  is identical to pure liquid  $\text{Cu}_2\text{O}$ . The linearity expected from equation 5.5 is observed in Figure 2 for activities of copper less than or equal to 0,8 in the copper-gold alloy.

#### 5.1.2 Activity of $\text{CuO}_{0,5}$

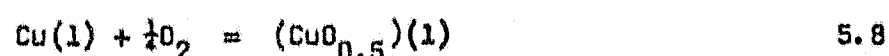
If it is assumed that copper dissolves in the slag as  $\text{Cu}^+$  ions the solubility of copper can be related to both the activity of copper oxide and the oxygen potential as follows

$$a_{\text{CuO}_{0,5}} = \gamma_{\text{CuO}_{0,5}} N_{\text{CuO}_{0,5}} \quad 5.7$$

where  $\gamma_{\text{CuO}_{0,5}}$  = activity coefficient of copper oxide

$N_{\text{CuO}_{0,5}}$  = mole fraction of copper oxide.

Now



therefore

$$a_{\text{CuO}_{0,5}}(1) = K a_{\text{Cu}(1)} P_{\text{O}_2}^{\frac{1}{2}} \quad 5.9$$

where (at  $1573^\circ \text{K}$ )  $K_{5,8} = 7,7045$  (refer Appendix)

The activity of copper (relative to pure liquid metal) in the liquid Cu-Au-Fe alloy was assumed to be the same as its activity in the binary Cu-Au alloy. In the majority of cases throughout the experimental programme the iron content of the alloy was less than 0,10 mass per cent and adjustments to the copper activity were considered unnecessary.

Activities in the liquid Cu-Au binary system have been determined by Oriani (48) at  $1258^\circ \text{K}$  from galvanic cell measurements

and by Edwards and Brodsky (34) at 1550° K using Knudsen weight loss measurements. Although the results of these investigations are consistent, the results appear to be incorrect in view of later work by Hultgren et al (49), Neckel and Wagner (50), Schmahl and Minzl (51), and Hager et al (35). The results of Edwards and Brodsky (incorporating extrapolated measurements of Oriani) (34) are unusual in that  $a_{Cu}$  shows a large negative deviation from ideal behaviour in the dilute solution range, but has a positive deviation for mole fractions of copper greater than 0.8. Partial molar heats of mixing are also subject to a large error because of the narrow temperature range over which the activity coefficients are measured. The activities of copper have therefore been estimated by linear interpolation at 1573° K from the work of Hager et al over the temperature range 1300° K to 1733° K. These values are compared with the values of Edwards and Brodsky in Figure 12.

Using equation 5.9 the activity of  $CuO_{0.5}$  was calculated for the alloy and slag compositions given in Table 4.2. The activity coefficient of copper oxide was then calculated from the equation

$$\gamma_{CuO_{0.5}} = a_{CuO_{0.5}} / N_{CuO_{0.5}} \quad 5.10$$

The activity and activity coefficients of copper oxide are listed in Table 5.1. This table also includes the results of similar calculations for additions of magnesia, alumina and lime.

The activity coefficient of copper oxide is plotted against the mole fraction of copper oxide in Figure 22 for silica-saturated slag without fluxing additions. The overall analytical error in the

TABLE 5.1

ACTIVITIES AND ACTIVITY COEFFICIENT OF  $\text{CuO}_{0.5}$  FOR ALLOY AND SLAG

Alloy Composition				Slag Composition		
Run No.	Mass % Cu	$X_{\text{Cu}}$	$a_{\text{Cu}}$	$a_{\text{CuO}_{0.5}}$	$N_{\text{CuO}_{0.5}}$	$\gamma_{\text{CuO}_{0.5}}$
<u>NO ADDITIONS</u>						
12	19.68	0.434	0.20	0.0146	0.0056	2.6071
44	29.91	0.570	0.34	0.0248	0.0095	2.6105
10	42.55	0.697	0.53	0.0386	0.0165	2.3394
55	53.73	0.783	0.68	0.0495	0.0190	2.6053
7	68.73	0.872	0.82	0.0597	0.0234	2.5513
53	99.90	1.000	1.00	0.0729	0.0263	2.7719
<u>MAGNESIA ADDITIONS</u> (4 mass per cent MgO)						
13	18.98	0.421	0.185	0.0135	0.0049	2.7551
14	31.52	0.588	0.36	0.0262	0.0095	2.7579
15	45.31	0.720	0.57	0.0415	0.0129	3.2171
16	57.49	0.810	0.725	0.0528	0.0192	2.7500
17	69.87	0.878	0.83	0.0605	0.0236	2.8636
56	99.97	1.000	1.00	0.0729	0.0247	2.9514

TABLE 5.1 cont.

ACTIVITIES AND ACTIVITY COEFFICIENT OF  $\text{CuO}_{0,5}$  FOR ALLOY AND SLAG

Alloy Composition				Slag Composition		
Run No.	Mass % Cu	$X_{\text{Cu}}$	$a_{\text{Cu}}$	$a_{\text{CuO}_{0,5}}$	$N_{\text{CuO}_{0,5}}$	$\gamma_{\text{CuO}_{0,5}}$
<u>ALUMINA ADDITIONS</u> (4 mass per cent $\text{Al}_2\text{O}_3$ )						
19	55,73	0,796	0,70	0,0510	0,0189	2,6984
18	68,55	0,871	0,82	0,0597	0,0231	2,5844
<u>ALUMINA ADDITIONS</u> (8 mass per cent $\text{Al}_2\text{O}_3$ )						
24	17,97	0,405	0,175	0,0128	0,0052	2,4615
25	31,11	0,584	0,355	0,0259	0,0089	2,9101
26	42,50	0,727	0,58	0,0423	0,0141	3,0000
57	53,72	0,783	0,68	0,0495	0,0186	2,6613
28	57,97	0,817	0,735	0,0536	0,0198	2,7071
<u>LIME ADDITIONS</u> (4,5 mass per cent $\text{CaO}$ )						
38	18,80	0,418	0,185	0,0135	0,0044	3,0682
36	31,47	0,589	0,36	0,0262	0,0092	2,8478
37	40,82	0,682	0,505	0,0368	0,0143	2,5734
34	52,63	0,775	0,665	0,0485	0,0176	2,7557
33	69,52	0,876	0,83	0,0605	0,0198	3,0556

TABLE 5.1 cont. ACTIVITIES AND ACTIVITY COEFFICIENT OF  $\text{CuO}_{0,5}$  FOR ALLOY AND SLAG

Alloy Composition				Slag Composition		
Run No.	Mass % Cu	$X_{\text{Cu}}$	$a_{\text{Cu}}$	$a_{\text{CuO}_{0,5}}$	$N_{\text{CuO}_{0,5}}$	$\gamma_{\text{CuO}_{0,5}}$
<u>LIME ADDITIONS</u> (7,5 mass per cent CaO)						
50	18,53	0,414	0,185	0,0135	0,0032	4,2188
49	30,44	0,576	0,345	0,0251	0,0076	3,3026
52	40,40	0,678	0,50	0,0364	0,0115	3,1652
51	54,76	0,790	0,69	0,0503	0,0150	3,3533
45	66,79	0,862	0,805	0,0587	0,0178	3,2978
<u>LIME ADDITIONS</u> (10,5 mass per cent CaO)						
41	18,62	0,416	0,185	0,0135	0,0029	4,6552
40	31,42	0,587	0,36	0,0262	0,0073	3,5890
32	43,32	0,704	0,54	0,0393	0,0102	3,8529
39	56,03	0,798	0,705	0,0514	0,0135	3,8074
30	65,03	0,857	0,80	0,0583	0,0146	3,9932



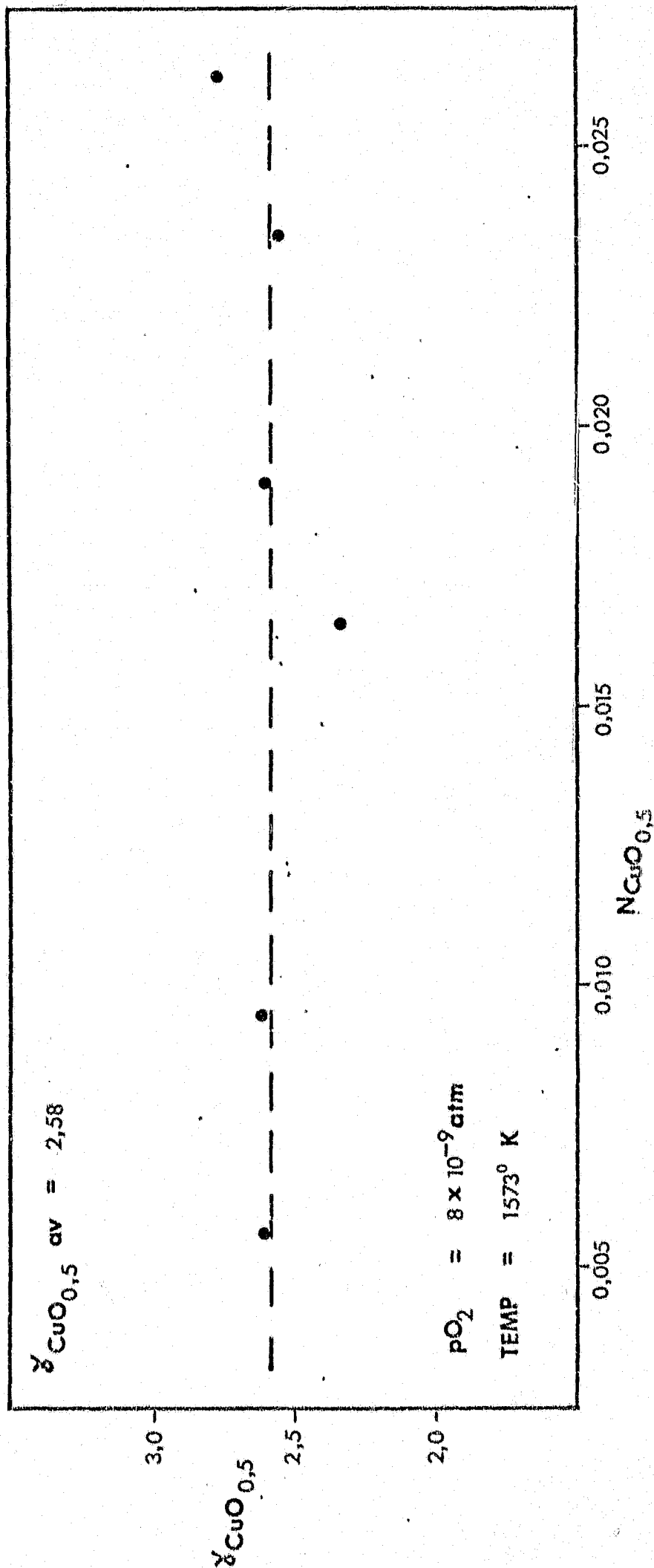


FIGURE 22 ACTIVITY COEFFICIENT OF COPPER OXIDE as a FUNCTION of MOLE FRACTION  
 of COPPER as COPPER OXIDE in SILICA - SATURATED SLAG  
 WITHOUT FLUXING ADDITIONS

sum of oxides present in the slag was of the order of  $\pm 5$  mass per cent. This would result in a maximum error in  $N_{\text{CuO}_{0,5}}$  of less than 0,5 per cent. The analytical error over this range has therefore been assumed to have a negligible effect on the activity coefficient of copper oxide. As may be seen from Figure 22, within the limits of experimental error the activity coefficient of  $\text{CuO}_{0,5}$  is constant and  $\text{CuO}_{0,5}$  exhibits Henrian behaviour over the range zero to 0,0263 mole fraction of  $\text{CuO}_{0,5}$ . The apparently constant value of  $\gamma_{\text{CuO}_{0,5}}$  over the range of mole fractions of copper oxide gave an average value of  $\gamma_{\text{CuO}_{0,5}} = 2,58$ . These observations support the view that soluble copper in the slag exists as the species  $\text{CuO}_{0,5}$ .

### 5.1.3 Prediction of Solubility of Copper

The solubility of copper oxide in silica-saturated iron silicate slag as a function of copper activity in the alloy can be predicted using the equation

$$a_{\text{CuO}_{0,5}} = K_1 a_{\text{CuPO}_2}^{\frac{1}{2}} \quad 5.4$$

$$= 0,07286 a_{\text{Cu}} \text{ at } 1573^\circ \text{ K} \quad 5.11$$

where  $K = 7,7045$  as calculated previously

$$\text{and where mass \% Cu in slag} \propto a_{\text{CuO}_{0,5}} \quad 5.6$$

The activity of copper oxide in the slag is plotted against  $a_{\text{CuO}_{0,5}}$  in Figure 23 and regression analysis was used to obtain the

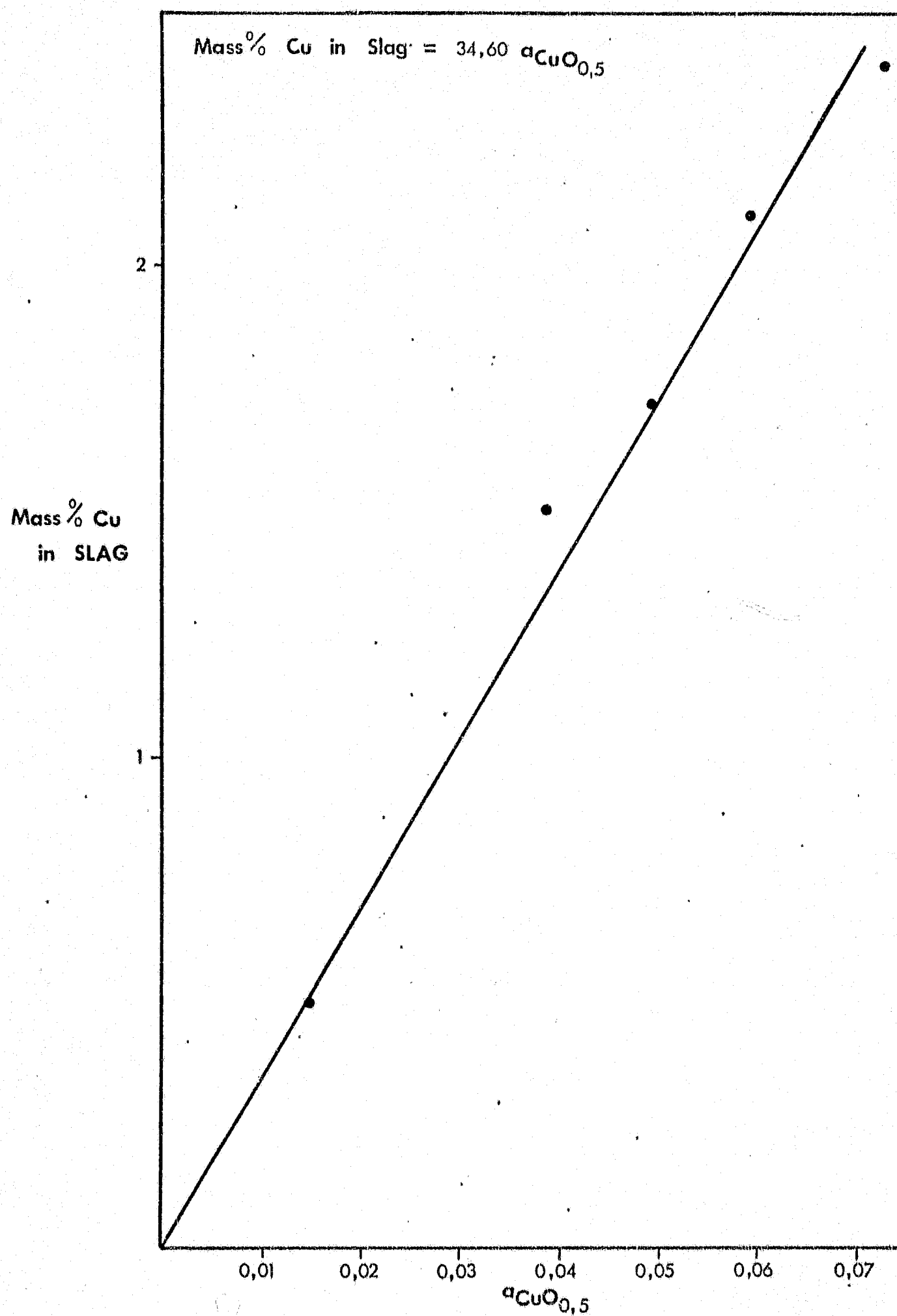


FIGURE 23

RELATIONSHIP BETWEEN MASS PER CENT COPPER  
OXIDE in SLAG and  $a_{\text{CuO}_{0,5}}$  at 1573° K for  
FLUX-FREE SILICA-SATURATED SLAG

relationship

$$\text{mass \% Cu in slag} = 34,60 a_{\text{CuO}_{0,5}} \quad 5.12$$

Analytical procedures give a  $\pm 2\%$  error in the raw data for copper solubility and thus it can be assumed that equation 5.12 predicts the solubility of copper in slag to within 3% over the solubility range zero to 2,4 mass per cent copper oxide.

Referring to Table 2.1 it can be seen that the results for copper solubility in silica-saturated slag for this investigation agree well with the results of Ruddie et al (8), Mihalop (15) and Altman and Kellogg (18) at  $1573^\circ \text{K}$  and a partial pressure of oxygen of  $10^{-8} \text{ atm}$ . The results of Toguxi and Santander (17) are somewhat lower and possibly due to the slag not being at silica saturation and to the effect of alumina in the slag. The results of Taylor and Jaffee (22) are slightly lower than the results for this investigation and this is possibly due to temperature fluctuations between the alloy and slag experienced when using the levitation technique.

## 5.2 Effect of Fluxing Additions

The solubility of copper in silica-saturated slags containing magnesia, alumina and lime is discussed in the following sections.

### 5.2.1 Magnesia

The solubility of copper in silica-saturated slag containing about 4 mass per cent magnesia is shown in Figure 24 as mass per

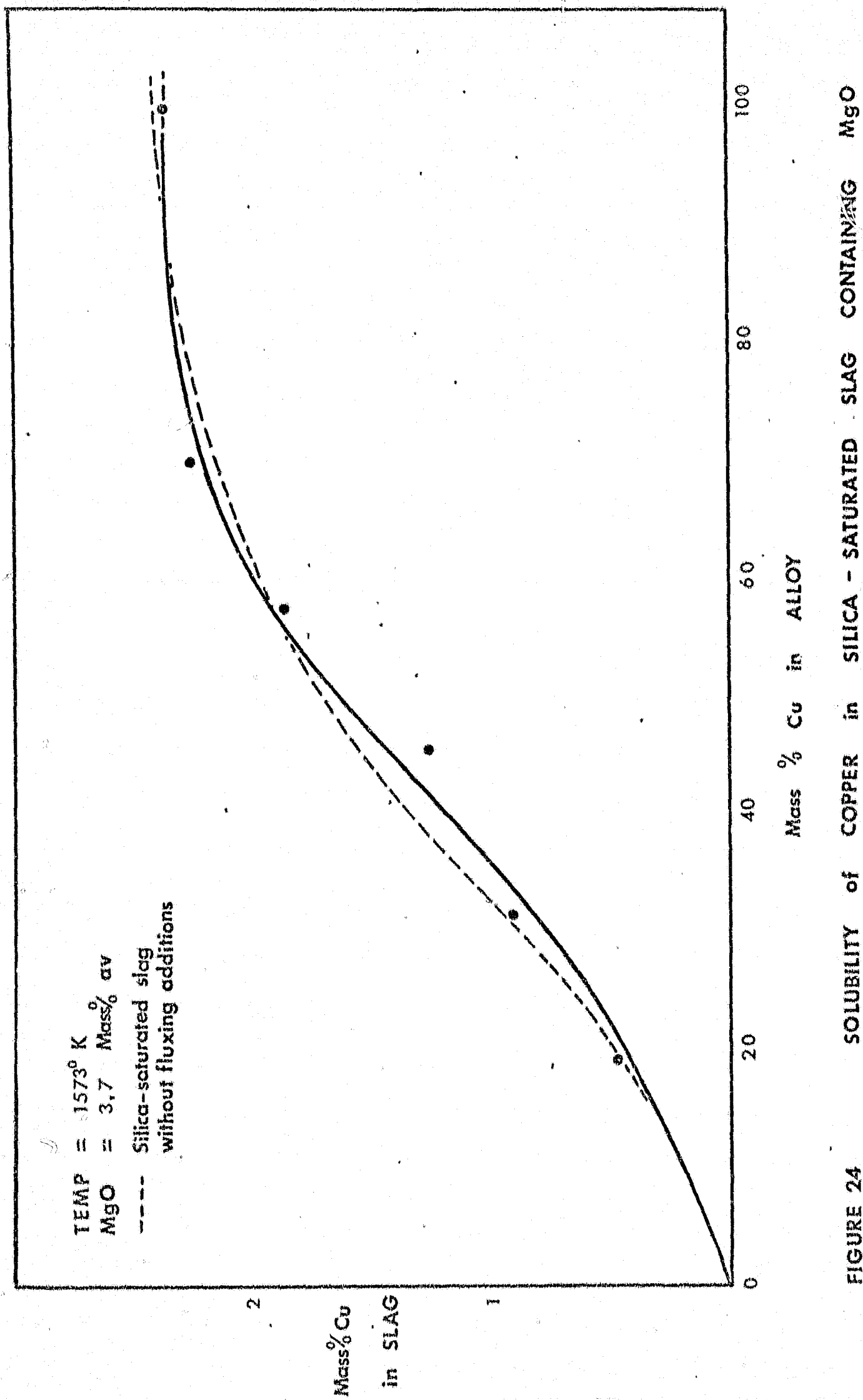


FIGURE 24 SOLUBILITY OF COPPER IN SILICA - SATURATED SLAG CONTAINING MgO

cent copper in the slag versus mass per cent copper in the alloy. The trend was similar to that observed for magnesia-free slags for which the copper solubility of the slag increased as the copper content of the alloy was increased (Figure 24). The copper content of the slag reached a maximum value of 2,2 mass per cent when the slag was equilibrated with pure copper.

The solubility data were analysed in a similar fashion to those for silica-saturated slags without fluxing additions and the results of the calculation of activity and activity coefficient of copper oxide are presented in Table 5.1. The activity coefficient of copper oxide is plotted against the mole fraction of copper oxide in Figure 25 and compared with the average value of activity coefficient for silica-saturated slags without fluxing additions. The apparently constant value of activity coefficient over the range of mole fraction of copper oxide from zero to 0,0247 indicates that Henry's law is obeyed. The average value of  $\gamma_{\text{CuO}_{0,5}}$  was 2,83.

The solubility of copper oxide in silica-saturated iron silicate slag containing 4 mass per cent magnesia as a function of copper activity in the slag can be predicted from the relationship

$$\text{mass \% Cu in slag} \propto a_{\text{CuO}_{0,5}} \quad 5.6$$

The relationship is plotted in Figure 26 and from regression analysis, obeys the equation

$$\text{mass \% Cu in slag} = 33,74 a_{\text{CuO}_{0,5}} \quad 5.13$$

which may be compared to the equation

$$\text{mass \% Cu in slag} = 34,60 a_{\text{CuO}_{0,5}} \quad 5.12$$

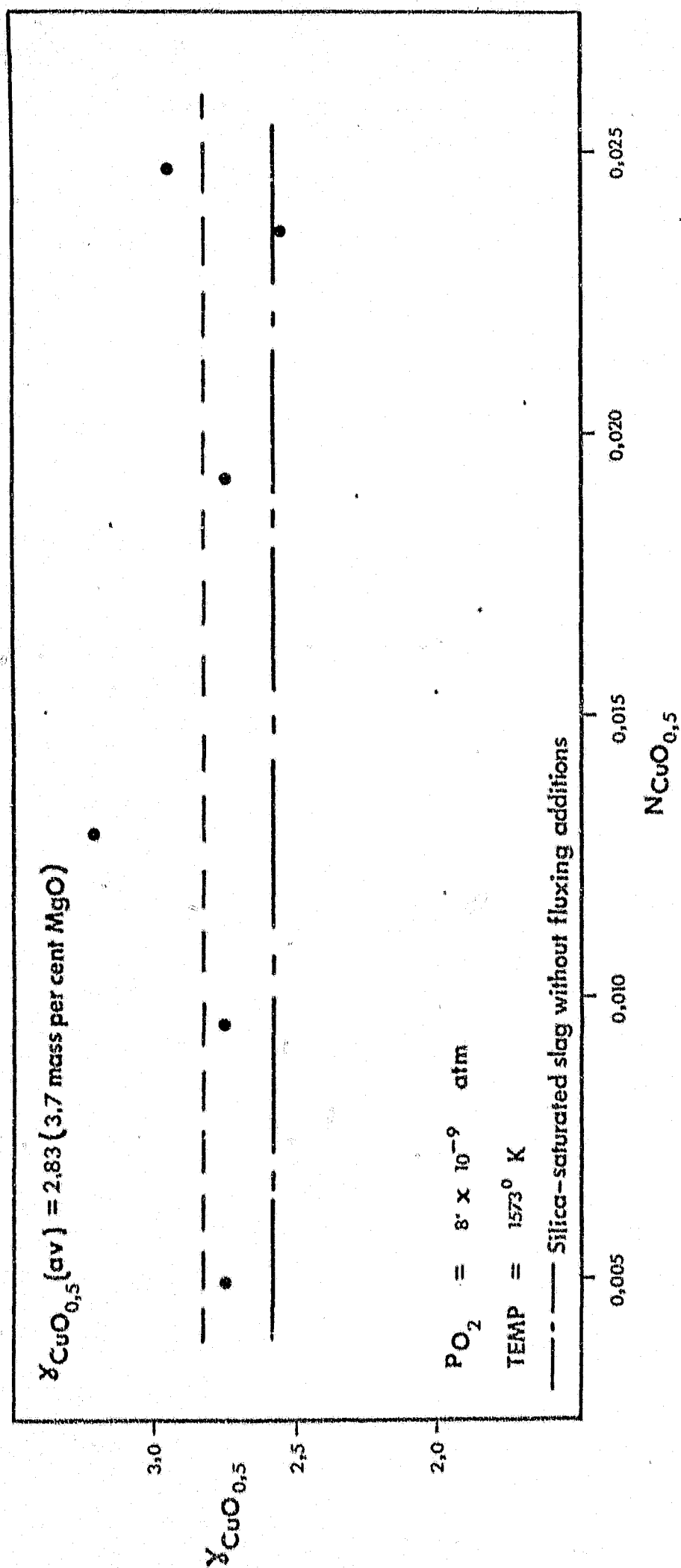


FIGURE 25 ACTIVITY COEFFICIENT OF COPPER OXIDE as a FUNCTION of MOLE FRACTION of COPPER OXIDE in SILICA - SATURATED SLAG CONTAINING 4 MASS PER CENT MgO

Mass% Cu  
in Slag

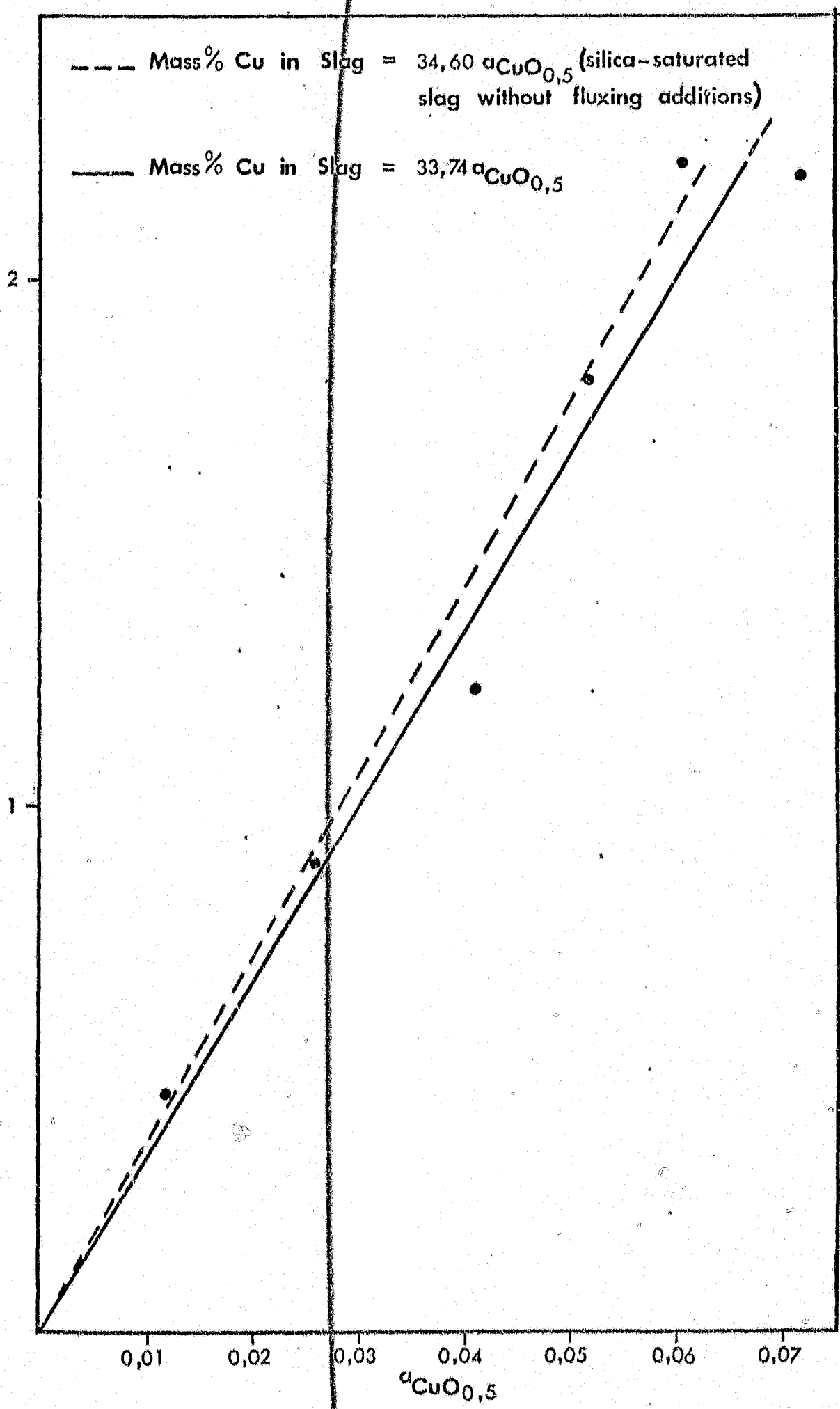


FIGURE 26

RELATIONSHIP BETWEEN MASS PER CENT COPPER and  $a_{\text{CuO}_{0,5}}$   
in SILICA-SATURATED SLAG CONTAINING 4 MASS PER CENT  
MgO at 1573° K



obtained for silica-saturated slags without fluxing additions. There is insufficient information on copper solubility in iron silicate slags containing magnesia available in the literature for comparison with this study.

The effect of additions of 4 mass per cent magnesia on the solubility of copper in silica-saturated iron silicate slags is not immediately obvious from Figure 24. However equation 5.14 shows that there is a slight decrease in the solubility of copper in slag containing 4 mass per cent magnesia by comparison with equation 5.12 for magnesia-free slag. The activity coefficient of copper oxide increased (Figure 25) for slag containing magnesia and the explanation for this and the lower solubility of copper in slag containing magnesia lies in the acid-base theory of slags (52).

Slag components may be classified as acid, basic or amphoteric. For acidic oxides, the cation-oxygen bonds are considerably stronger than those of basic oxides. For three-dimensional silica structures the cation enters a hole in which it is co-ordinated with twelve oxygen ions. An increase in the co-ordination of the cation to a point where it is just in contact with the surrounding oxygen ions increases the length of the cation-oxygen bonds and raises the energy of the system, thus making the structure less stable. The degree of instability is raised as the cation-oxygen bond strength is increased in the pure basic oxide and as the size of the basic oxide cation is decreased.

The ion-oxygen attraction  $F$  between a cation of valency  $Z^+$  and an anion of valency  $Z^-$  may be expressed as (52)

$$F = \frac{Z^+ Z^- e^2}{r^2} \quad 5.14$$

where  $e$  is the electron charge and  $r$  is the mean distance of separation between the centres of the ions. Calculated values of  $F/e^2$  for various oxides are compared below and used as a basis for the division of the oxides into basic, acidic or amphoteric (53).

TABLE 5.2 ACID-BASE CLASSIFICATION OF OXIDES (53)

Oxide	$F/e^2$	Classification
$\text{Na}_2\text{O}$	0,36	basic
$\text{BaO}$	0,53	
$\text{Cu}_2\text{O}$	0,60	
$\text{CaO}$	0,70	
$\text{MnO}$	0,83	
$\text{FeO}$	0,86	
$\text{ZnO}$	0,87	amphoteric
$\text{MgO}$	0,95	
$\text{Fe}_2\text{O}_3$	1,44	
$\text{Al}_2\text{O}_3$	1,66	acid
$\text{TiO}_2$	1,85	
$\text{SiO}_2$	2,44	
$\text{P}_2\text{O}_5$	3,31	

The classification of oxides in slag depends on the composition of the slag itself. For slags which are acidic in nature the amphoteric oxides tend to act as basic oxides and in basic slags they act as acids.

In the liquid state the regular arrangement of the ions is destroyed (52) and the cation is free to interchange its position whilst remaining co-ordinated on the average with approximately the same number of anions as in the solid state. The mobility of the cations is related to its electron charge and co-ordination number. It is to be expected that cations of acid classification are less mobile than basic oxides and thus less likely to provide oxygen ions when dissolved in the slag.

From Table 5.2 silica is a very acidic oxide. In the liquid state, silica has a tetrahedron structure. When a basic oxide is added to liquid silica each oxygen ion enters the network and separates the corners of two tetrahedra whilst the added cation remains adjacent to the separation and is accommodated within the holes of the structures. With progressive additions of the basic oxide the three-dimensional array is steadily broken down to form silicate polymers (52).

The solubility of copper is determined by the availability of sites within the silicate structure which in turn is a function of slag composition. For iron silicate slags equilibrated with copper metal, copper oxide acts as a basic oxide (Table 5.2) and breaks the silicate structure to associate with oxygen anions. The

addition of copper to the slag should be reflected by a small change in the concentration of the amphoteric oxide  $\text{Fe}_2\text{O}_3$ . Such a small change would be shown by the  $\text{Fe}^{3+}/\text{Fe}^{2+}$  ratio. For copper-free slag  $\text{Fe}^{3+}/\text{Fe}^{2+} = 0,0811 \pm 0,01$  (19) at a partial pressure of oxygen of  $8 \times 10^{-9}$  atm, whilst for slag containing copper in this study  $\text{Fe}^{3+}/\text{Fe}^{2+} = 0,080 \pm 0,01$ . This difference is not significant.

Magnesia is an amphoteric oxide and in silica-saturated iron silicate slag acts as a basic oxide. The addition of 4 mass per cent magnesia should result in a slight decrease in the mass per cent copper in the slag. The copper content of the slag is seen to decrease slightly with the addition of  $\text{MgO}$  according to the relationships

$$\text{mass \% Cu in slag} = 34,60 \text{ }^{\circ}\text{CuO}_{0,5} \quad 5.12$$

(silica-saturated slag without  
fluxing additions)

$$\text{mass \% Cu in slag} = 33,74 \text{ }^{\circ}\text{CuO}_{0,5} \quad 5.13$$

(containing 4 mass %  $\text{MgO}$ )

The  $\text{Mg}^{2+}$  and  $\text{Cu}^+$  ions in the two basic oxides,  $\text{CuO}_{0,5}$  and  $\text{MgO}$ , will be mobile within the silicate structure and therefore it can be assumed that a small percentage of the sites within the silica structure occupied by copper ions will be replaced by magnesia ions and the solubility of copper in the slag will be reduced. There should also be a slight decrease in the  $\text{Fe}^{3+}/\text{Fe}^{2+}$  ratio because  $\text{Fe}_2\text{O}_3$  is less basic than magnesia. This was not observed in the

results as  $\text{Fe}^{3+}/\text{Fe}^{2+} = 0,080 \pm 0,01$  for silica-saturated slag without fluxing additions and  $\text{Fe}^{3+}/\text{Fe}^{2+} = 0,083 \pm 0,01$  for slag containing  $\text{MgO}$ . This effect is thought to be due to analytical error resulting from the small sample sizes and the difficulty in the analysis of  $\text{FeO}$ .

### 5.2.2 Alumina

The solubility of copper in silica-saturated slag containing about 8 mass per cent alumina is shown in Figure 27. Although the scatter in the results makes comparison difficult, it appears that the addition of 8 mass per cent alumina decreased the solubility of copper in silica-saturated slag very slightly for copper contents of up to 60 mass per cent in the Cu-Au alloy. The copper content of the slag reached a maximum value of 1,845 mass per cent when the slag was equilibrated with a copper-gold alloy containing 58 mass per cent copper.

Additional runs were conducted with slags containing about 4 mass per cent alumina. These results have been included in Figure 27. There appears to be very little difference between the results for 4 mass per cent and 8 mass per cent alumina which implies that alumina has very little effect on the solubility of copper in silica-saturated slags up to 8 mass per cent alumina.

The calculated activities and activity coefficients of copper oxide are presented in Table 5.1 and the activity coefficient of

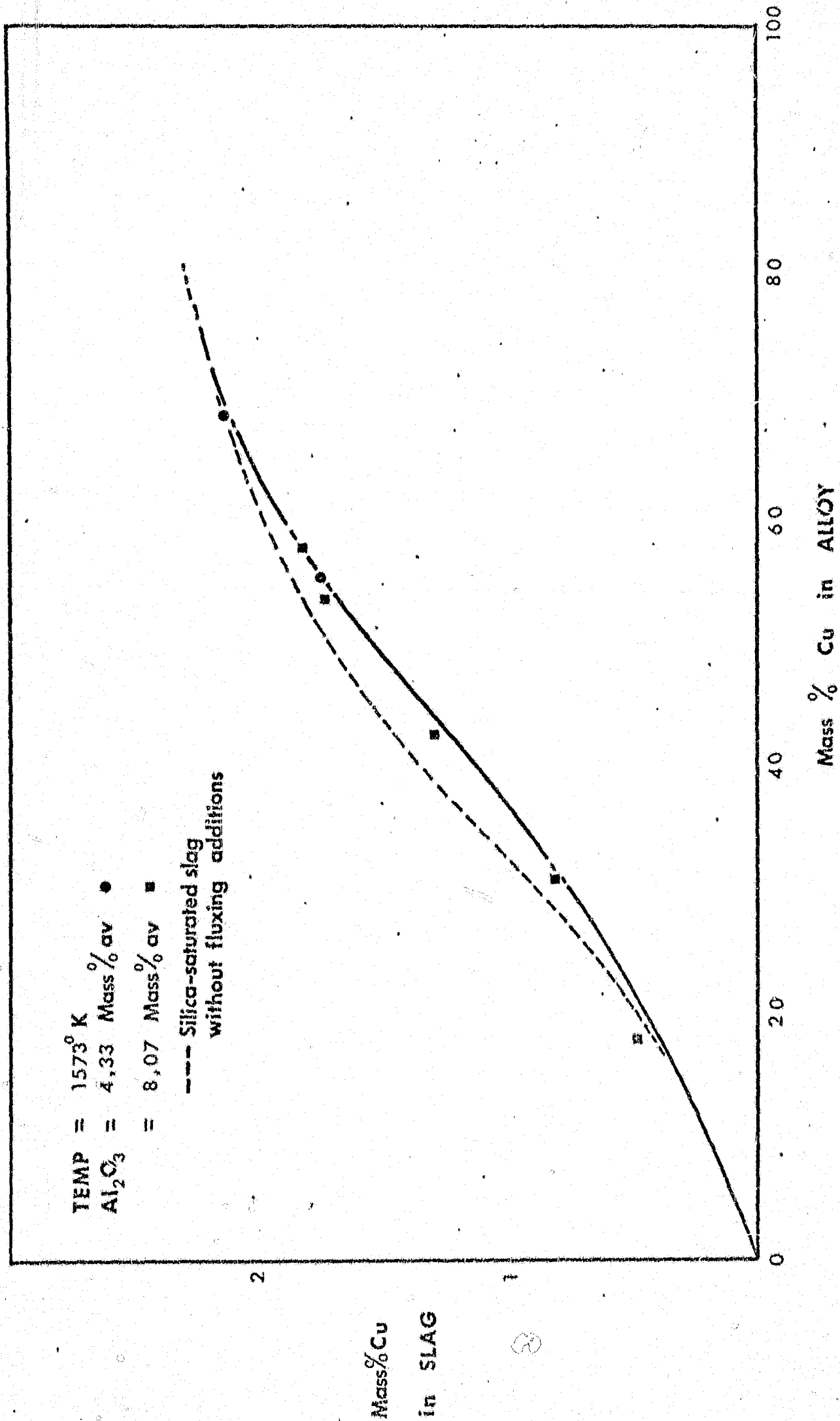


FIGURE 27 SOLUBILITY OF COPPER IN SILICA-SATURATED SLAG CONTAINING Al<sub>2</sub>O<sub>3</sub>

copper oxide is plotted against the mole fraction of copper oxide in Figure 28. From this figure it can be seen that the addition of 8 mass per cent alumina to the slag increases  $\chi_{\text{CuO}_{0,5}}$  from 2,58 for alumina-free slags to 2,75.

For silica-saturated iron silicate slags containing 8 mass per cent alumina, the relationship

$$\text{mass \% Cu in slag} \propto a_{\text{CuO}_{0,5}} \quad 5.6$$

is plotted in Figure 29 and produces the equation

$$\text{mass \% Cu in slag} = 34,18 a_{\text{CuO}_{0,5}} \quad 5.15$$

which is comparable to equation 5.12 for alumina-free slag

$$\text{is } \text{mass \% Cu in slag} = 34,60 a_{\text{CuO}_{0,5}} \quad 5.12$$

As may be seen by comparing equations 5.18 and 5.13 the addition of 8 mass per cent alumina to the silica-saturated slag depresses the solubility of copper oxide slightly compared to the value of this solubility for a silica-saturated slag without fluxing additions.

This slight reduction in the solubility of copper may be explained from the acid-base theory of slags. From Table 5.2 it can be seen that  $\text{Al}_2\text{O}_3$ , like  $\text{MgO}$ , is an amphoteric oxide and thus acts as a basic oxide in silica-saturated iron silicate slag. Alumina is less basic than magnesia and thus its effect in lowering the solubility of copper should be less pronounced for the same concentration of flux. The effect of alumina is less than that of magnesia (4 mass per cent) even at a concentration of 8 mass per cent.

When 8 mass per cent  $\text{Al}_2\text{O}_3$  is added to the slag, the value of the  $\text{Fe}^{3+}/\text{Fe}^{2+}$  ratio was  $0,074 \pm 0,01$  compared to the value of

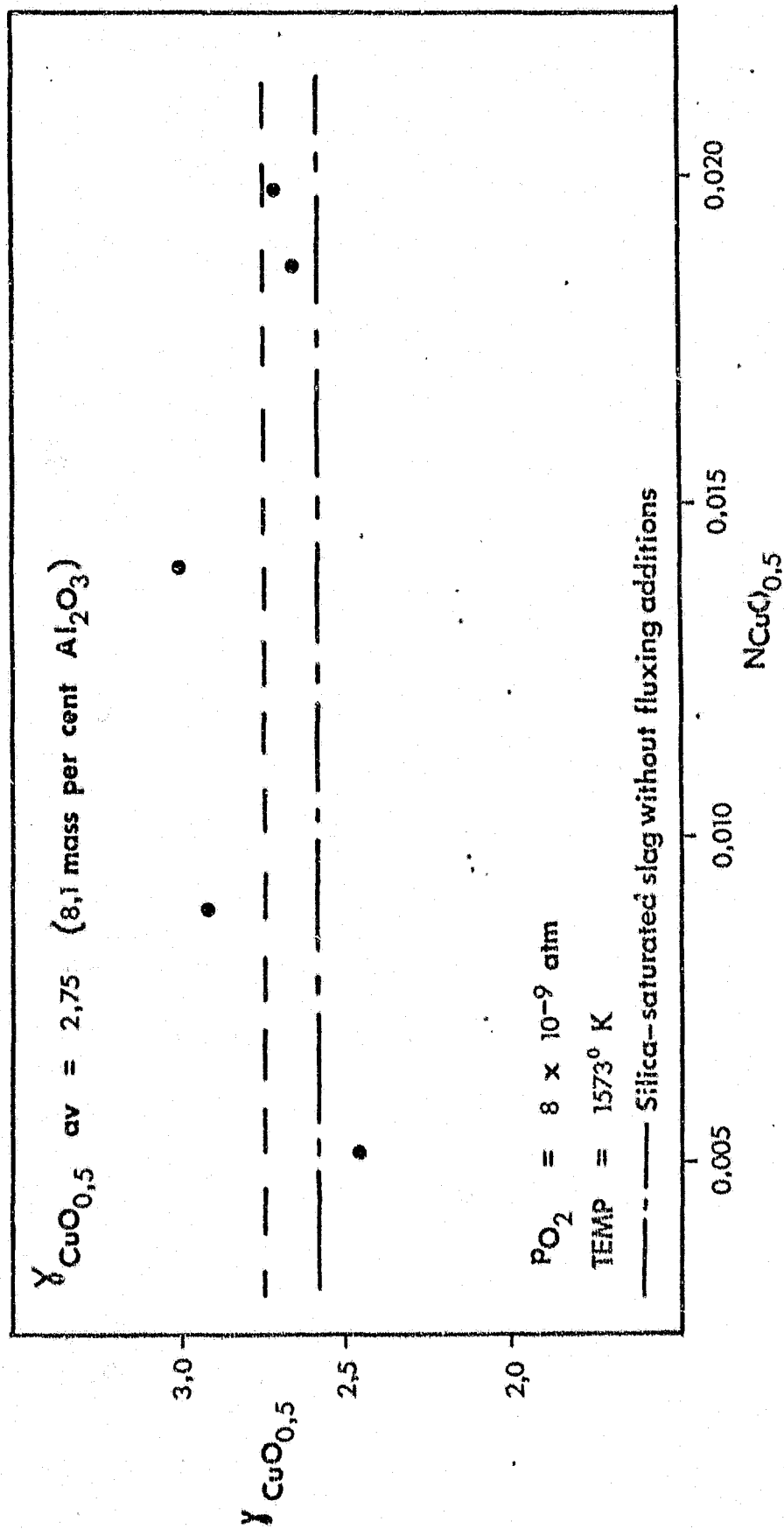


FIGURE 28  
 ACTIVITY COEFFICIENT OF COPPER OXIDE as a FUNCTION of  
 MOLE FRACTION of COPPER OXIDE in SILICA-SATURATED  
 SLAG CONTAINING ALUMINA



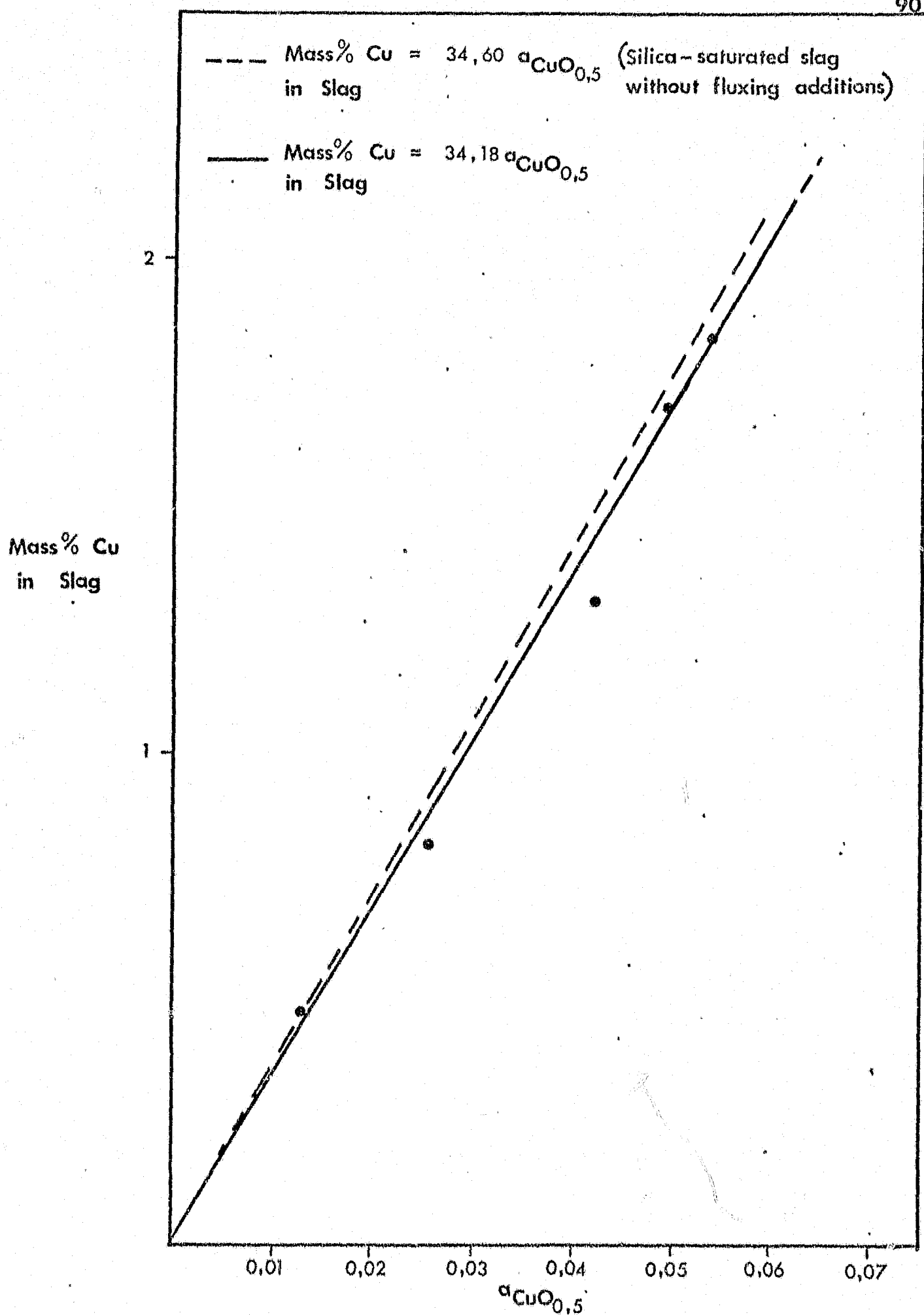


FIGURE 29

RELATIONSHIP BETWEEN MASS PER CENT COPPER and  $a_{\text{CuO}_{0,5}}$  in SILICA-SATURATED SLAG CONTAINING 8 MASS PER CENT  $\text{Al}_2\text{O}_3$  at 1573° K

**Author** Elliot B J

**Name of thesis** The effect of Slag composition on Copper losses to Silica-saturated Iron Silicate Slags 1977

***PUBLISHER:***

University of the Witwatersrand, Johannesburg

©2013

***LEGAL NOTICES:***

**Copyright Notice:** All materials on the University of the Witwatersrand, Johannesburg Library website are protected by South African copyright law and may not be distributed, transmitted, displayed, or otherwise published in any format, without the prior written permission of the copyright owner.

**Disclaimer and Terms of Use:** Provided that you maintain all copyright and other notices contained therein, you may download material (one machine readable copy and one print copy per page) for your personal and/or educational non-commercial use only.

The University of the Witwatersrand, Johannesburg, is not responsible for any errors or omissions and excludes any and all liability for any errors in or omissions from the information on the Library website.